

## Shunts in crystalline silicon PV modules: A comprehensive review of investigation, characterization, and mitigation

Ravi Kumar, Rajesh Gupta\*

Department of Energy Science and Engineering, Indian Institute of Technology Bombay Mumbai-400076, India



### ARTICLE INFO

**Keywords:**  
 Photovoltaic cell  
 Shunt defect  
 Shunting mechanism  
 Shunt characterization  
 Modeling  
 Prevention  
 Mitigation

### ABSTRACT

Shunts in solar cells significantly affect their performance and reliability, potentially leading to hotspot generation and long-term module failure. Investigating shunts is essential for enhancing solar cell power output and preventing efficiency losses. While extensive research has been conducted on the investigation, characterization, and mitigation of shunts, a consolidated review is necessary to identify optimal techniques and highlight research gaps. This paper provides a comprehensive review of shunts in solar cells, examining their effects on performance and reliability, and exploring various characterization and mitigation strategies. The review categorizes different shunt mechanisms, detailing their origins, characteristics, and impact on performance. It critically evaluates various characterization techniques, classifying them as destructive/non-destructive and spatial/non-spatial, and discusses their advantages and limitations. The paper also highlights advancements in technologies such as luminescence and lock-in thermography, which offer qualitative and quantitative insights into shunts. Additionally, it compares various electrical and thermal models used to study the spatial impact of shunts, assessing their accuracy and suitability. The review further examines reported mitigation techniques, summarizing their effectiveness, targeted applications, and associated challenges. Overall, this paper provides a detailed overview of the progress in detecting, characterizing, modeling, and mitigating shunts, and offers insights into future prospects for improving solar cell efficiency and reliability.

### Abbreviations

(continued)

APT	Atomic Probe Tomography	PDLC	Polymer Dispersed Liquid Crystal
CCD	Charge Coupled Device	PV	Photovoltaic
DLIT	Dark Lock-in Thermography	PL	Photoluminescence
DDM	Double Diode Model	QUEL	Quantitative Electroluminescence
EDX	Energy Dispersive X-ray	RAMP	Resistance Analysis by Mapping of Potential
EL	Electroluminescence	SEM	Scanning Electron Microscopy
EBIC	Electron Beam Induced Current	SDM	Single Diode Model
FMI	Fluorescent Microthermal Imaging	TEM	Transmission Electron Microscopy
FF	Fill Factor	TOF-SIMS	Time-of-Flight Secondary Ion Mass Spectrometry
GHG	Green House Gas	UV	Ultraviolet
g-QUEL	Generalized Quantitative Electroluminescence	Nomenclature	
ILIT	Illuminated Lock-in Thermography	Al	Aluminum
IR	Infrared	c	Crystalline
IEA	International Energy Agency	V	Voltage
IR <sub>INV</sub>	Inverse Infrared	V <sub>oc</sub>	Open Circuit Voltage
LIT	Lock-in Thermography	I <sub>0</sub>	Saturation Current
LASER	Light amplification by stimulated emission of radiation	Na	Sodium
Nd:YAG	Neodymium-doped Yttrium Aluminum Garnet	R <sub>sh</sub>	Shunt Resistance
PID-s	Potential Induced Degradation-Shunting	Si <sub>3</sub> N <sub>4</sub>	Silicon Nitride
		Ag	Silver

(continued on next column)

(continued on next page)

\* Corresponding author.

E-mail addresses: [ravikr@iitb.ac.in](mailto:ravikr@iitb.ac.in) (R. Kumar), [rajeshgupta@iitb.ac.in](mailto:rajeshgupta@iitb.ac.in) (R. Gupta).

(continued)

mc	Multi-crystalline
I	Current
$I_{sc}$	Short Circuit Current
$P_{max}$	Maximum Power
n	Ideality Factor
Si	Silicon
TWh	Terawatt Hour

## 1. Introduction

Electricity is one of the basic needs of human society, and due to the increasing population and advanced daily activities, the demand for electricity is constantly rising. The net contribution of renewable sources to the world's total electricity generation is increasing day by day and has reached almost 30 % of total electricity generation in 2022 [1]. Among these sources, solar photovoltaic (PV) plays a pivotal role with 1300 TWh electricity production as of 2022 [2]. The solar cell is the basic unit of the PV system, essentially a diode of large area compared to its thickness. Under incident solar radiation of energy equal to or greater than the band gap, the solar cell generates current and voltage. The performance of the PV system depends on the cell characteristics and ambient conditions [3]. One major target is to improve the performance of PV technology under actual outdoor conditions for a service life of 25–30 years. However, several defects and degradations occur in this technology, affecting performance and reliability, thus raising serious concerns [4–7]. Defects may arise during the manufacturing of solar cells and modules or during field operations. The International Energy Agency (IEA) has reported a wide variety of commonly occurring defects in PV modules [8]. Shunt is one of the most commonly observed defects in solar cells and modules, causing serious concern [9–12].

A shunt is a parallel high-conductivity path across the p-n junctions or at the cell edges, causing unwanted short-circuit current flow between the junctions [13]. In the conventional understanding of a solar cell's current-voltage ( $I-V$ ) characteristics, the non-linear current is typically associated with the cell itself, while only the ohmic current paths across the junction are considered responsible for shunting. However, further studies have found that some shunts are local recombination sites that show non-linear behavior [14]. Shunts lead to leakage current from emitter to the base layer and divert light-generated current away from the intended load as depicted in Fig. 1. This current diversion results in a decrease in the current passing through the solar cell and lowers the cell's voltage. Shunts affect the open circuit voltage ( $V_{oc}$ ) and fill factor (FF), and hence the net power output ( $P_{max}$ ) of the PV cell reduces [10, 15]. The impact of shunt resistance intensifies under low light conditions, given the diminished amount of light-generated current in such scenarios [16].

Breitenstein et al. [9,17–25] have extensively investigated different types of shunts in crystalline silicon technology using lock-in thermography (LIT) and electroluminescence (EL) imaging techniques, categorizing them into process-induced and material-induced shunts. Few studies found shunts in the field due to hotspots and potential stress [6,

26,27]. Naumann et al. [28–34] have investigated potential-induced degradation shunting (PID-s) in great detail using microstructural characterization techniques. Different destructive/non-destructive and spatial/non-spatial characterization techniques have been reported in various literature with the development of new techniques over time [19,23,33,35–37]. To study the spatial and severity impact of shunts on performance and reliability, various electrical and thermal models have been reported in the literature. Various mitigation strategies for different types of shunts have been reported in the literature [12,15, 38–41]. However, there is a need for an extensive review summarizing the origins, characterization, modeling, and mitigation of shunts reported in various literature at one place. The extensive review will help researchers and industries to understand the basis of precautionary measures based on the nature, origin, and severity of shunts, ultimately aiding in minimizing shunt effects in cells and modules.

This paper presents a comprehensive review of research concerning shunts aimed at identifying optimal characterization and mitigation techniques, while also pinpointing research gaps for further exploration. Various shunt mechanisms are categorized and detailed regarding their origin, key characteristics, and impact on performance. The paper critically examines and summarizes different characterization techniques, categorizing them as destructive/non-destructive and spatial/non-spatial, along with their respective advantages and disadvantages. Also, it focuses on current advancements in characterization methodologies, both qualitative and quantitative, for obtaining information regarding the nature and severity of shunts. Typically, a modeling approach is utilized to study the spatial impact of shunts on solar cell performance. This work compares various electrical and thermal models of shunts in terms of their capabilities, accuracy, and suitability. Shunts in PV modules present a significant challenge to solar cell performance and reliability. This comprehensive review enhances understanding of shunt detection and characterization, providing valuable insights into mitigation and prevention strategies crucial for improving overall efficiency and reliability of solar cells. Furthermore, the paper presents summarized tables detailing shunt types, characterization techniques, modeling approaches, and prevention/mitigation methods.

The rest of the article is organised as follow. Section 2 provides overview of shunt formation and types, which sets the foundation for subsequent discussions. Section 3 examines the reported methods for shunt detection and characterization, distinguishing between destructive and non-destructive methods techniques. Studies employing destructive methodologies such as Scanning Electron Microscopy (SEM), Transmission Electron Microscopy (TEM), Atomic Probe Tomography (APT), and Electron Beam Induced Current (EBIC) are presented. Non-destructive methods, encompassing spatial and non-spatial characterization techniques, are emphasized, with a detailed analysis of LIT and luminescence imaging. In Section 4, investigation of shunt effects on PV cell performance and reliability is presented. Various methods are reviewed for quantifying the impact of shunting on parameters like  $V_{oc}$ , FF, and  $P_{max}$ . Modeling and simulation techniques, particularly distributed electrical modeling and thermal modeling, are presented as effective tools to assess the spatial and thermal effects of shunts. Section 5 presents the strategies for shunt prevention and mitigation. The section examines advancements in cell fabrication techniques, highlighting the detrimental effects of poor edge isolation. Mitigation strategies include physically removing shunted regions and the employing bypass diodes in partial shading scenarios. Advanced edge isolation techniques, such as laser-doped and laser isolation methods, are presented, focusing on their efficacy in enhancing cell efficiency. Prevention strategies for PID-s at the system, module, and cell levels are outlined. Finally, Section 6 summarizes the paper and outlines future prospects.

## 2. Origin and mechanism of shunt

Different types of shunts have been investigated in the literature. The nature of the shunts differs either by linear or non-linear  $I-V$

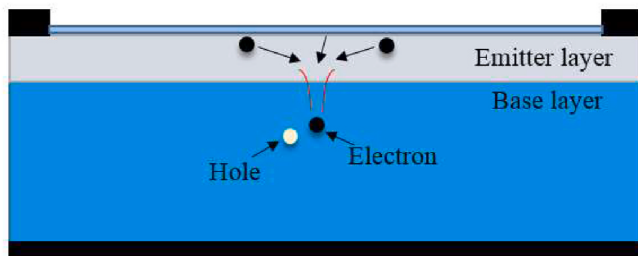


Fig. 1. Shunt in a solar cell.

characteristics, categorized as linear or non-linear shunts, or by origination, for example, due to issues related to materials or processes, they are classified as material-induced shunts and process-induced shunts, respectively [9,18,42]. Weak localized regions in solar cells with higher breakdown voltage compared to nearby regions have also been categorized as a type of non-linear shunt, termed as 'pre-breakdown sites' [25]. Earlier studies assumed that majority of the shunts in mc-Si solar cells could originate due to crystallographic defects in cells, such as grain boundaries, dislocations, or precipitates. Breitenstein et al. [9] extensively investigated the presence of shunts in more than a hundred commercial mono and multi-crystalline silicon solar cells. The study revealed that most of the shunts are caused by processes, while shunts induced by materials are relatively lower. The study has identified nine different shunt types based on physical origin, of which six types are process-induced, and three are material-induced.

In addition to these process-induced and material-induced shunts, shunts can also be induced due to shading and hotspot heating, temperature and humidity stress, or due to high potential stress on a PV cell in a string, as shown in Fig. 2.

### 2.1. Process-induced shunts

Process-induced shunts includes shunts at edges, shunts due to cracks, Schottky-type shunts, shunts due to Al inclusion, and shunts due to scratches, as shown in Fig. 3.

Roy and Gupta [43], investigated shunt types in a large set of commercial c-Si PV modules and categorized the shunts based on their spatial locations in the cells, as depicted in Fig. 4.

The most common types of shunts were found at the corners and edges of the cells, which are related to faults due to a poor edge isolation process. It is a common manufacturing fault, also in agreement with the most commonly observed edge shunts by Breitenstein et al. [9,17]. The poor quality of metallic junction removal at the corners and edges leads to leakage paths (shunts) in those regions. The incompletely opened emitter layer at the corners and edges that creates a shunting effect generally shows linear *I-V* characteristics. However, in some cases, the p-n junctions at the corners and edges become recombination centers and show non-linear *I-V* characteristics [44]. Their recombination current exhibits exponential characteristics in most cases [24]. Both linear and non-linear edge shunts are depicted in Fig. 3(a), with the white arrow indicating linear shunts.

Another type of shunts appears due to cracks: if cracks exist in the

wafer prior to cell processing or emerge during processing, it may lead to ohmic shunts. The front contact metallization (busbars and fingers) in solar cells is typically formed using screen printing technology [45]. In most cases during the screen-printing process, metal paste penetrates through the crack, resulting in strong ohmic shunts as shown in Fig. 3(c). Generally, Ag is used as the metallization material for its high conductivity, solderability, and low diffusion coefficient in silicon [46]. During this process, the Ag paste is systematically deposited at a higher temperature process called 'contact firing' [47], to make ohmic contact between the deposited metal and the semiconductor. Under a non-optimized contact firing process, Ag material may penetrate through the p-n junction at localized regions in the cell, leading to localized ohmic shunts, termed as 'metallization shunts', shown in Fig. 3(b). Some studies have shown the appearance of shunts under fingers and busbars in the cells of PV modules [40,43,48].

The Schottky-type shunts appear due to the improper optimization of the metallization parameters with the doping profile of the emitter layer [9]. This leads to the formation of a Schottky-type direct connection between the metal and the p-type base material. Such shunts may also occur when the metallization layer is applied in a location lacking the emitter layer entirely.

Shunts can also occur because of surface scratches on a solar cell cutting across the emitter layer. This exposes the p-n junction to a surface with a high concentration of recombination centers, as depicted in Fig. 3(d). These types of shunts have non-linear *I-V* characteristics, or specifically exponential characteristics in most cases [9].

One of the common types of shunts is due to the presence of Al particles during cell processing. These particles appear due to contamination during cell stacking, contacting directly with the base layer of the cell, and resulting in strong ohmic shunts. Fig. 3(e) depicts the presence of Al particle at the shunted site [9].

### 2.2. Material-induced shunts

The crystallographic defects, such as grain boundaries or bulk defects, act as local recombination centers in solar cells. However, if the recombination current is severe enough, it leads to a shunting effect and is categorized as shunts resulting from strongly recombinative crystal defects as shown in Fig. 5(a). Additionally, cast multi-crystalline silicon material contains macroscopic inclusions, identified as the presence of  $\text{Si}_3\text{N}_4$  originating from the walls of the crucible used for crystallizing the silicon material. The recombination activity of interface states between

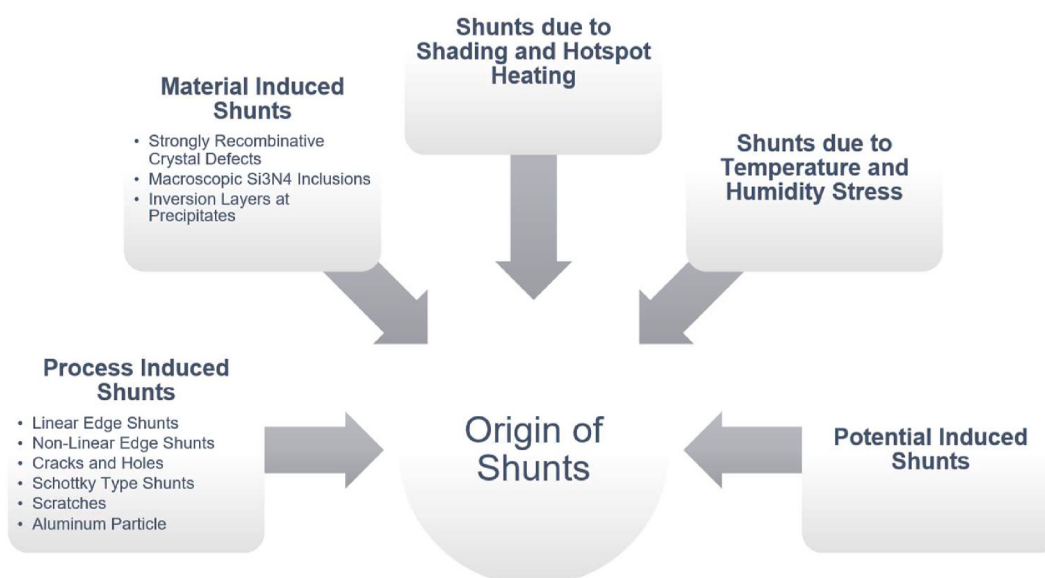
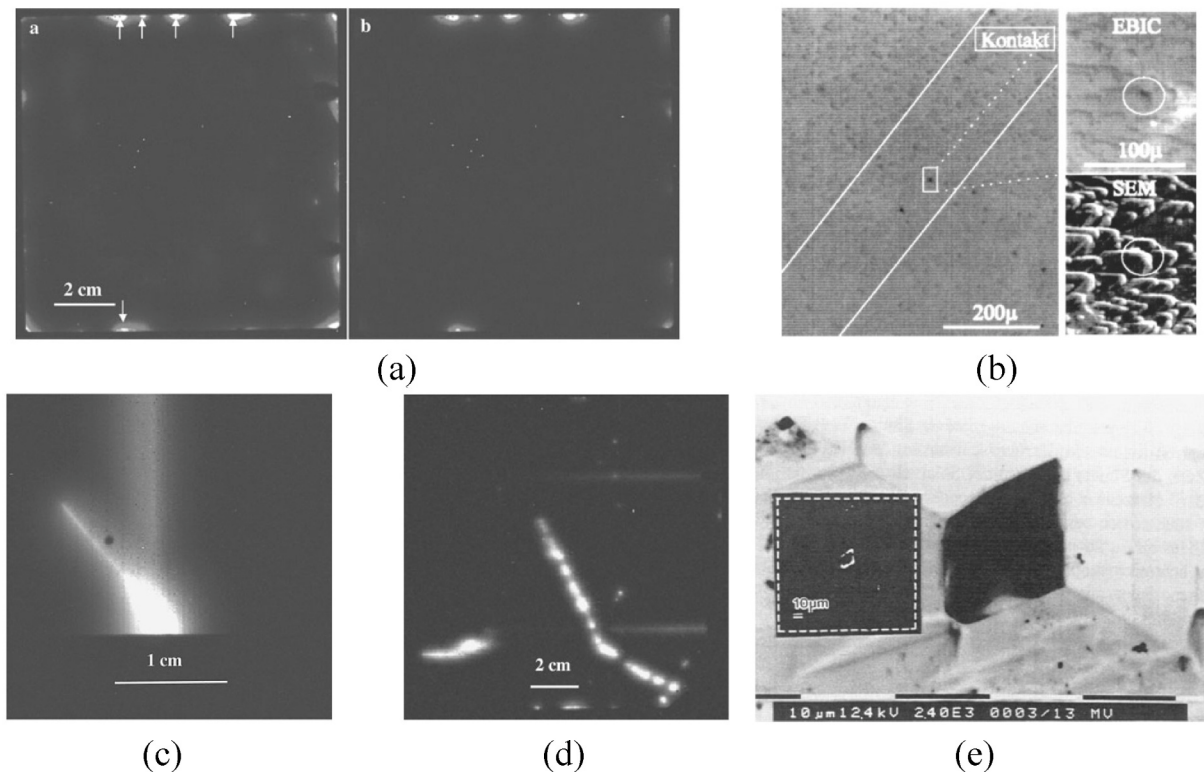
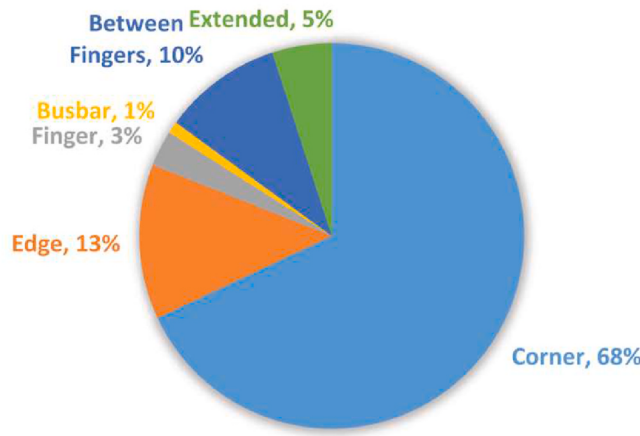


Fig. 2. Different origins of shunts in c-Si PV cells/modules.



**Fig. 3.** Process induced shunts (a) linear and non-linear edge shunts (b) shunt below metal grid (c) shunts at cracked sites (d) shunts at scratches (e) Al-induced shunts [9].



**Fig. 4.** Frequency of different shunt locations [43].

Si and  $\text{Si}_3\text{N}_4$  leads to a shunting effect as shown in Fig. 5(b). The inversion layer type of material-induced shunts is formed due to a local transformation of the silicon material from p to n-type, caused by the presence of fixed positive charges in the large-angle grain boundaries present in silicon material. This causes electrically connected channels from the emitter to the base layer and sometimes to the rear contact, resulting in a strong shunting effect as shown in Fig. 5(c) [9].

Some studies have investigated the physical origin of pre-breakdown sites [49–55]. The emergence of these sites may result from a localized rise in the electric field within the p-n junction, attributed to either the non-planar shape of the junction or the presence of voids in the material, resulting in elevated local fields. A similar effect may occur at localized junction regions with certain grain boundaries showing preferential P diffusion [56]. However, in most studies, the pre-breakdown sites have

mostly been considered as non-linear shunts only [25,57].

### 2.3. Shunts due to shading and hotspot heating

Partial shading is a commonly encountered phenomenon in PV modules. In the case of partial shading, the photo-generated current is reduced for a cell or a set of cells. Under series connection, the shaded cell becomes reverse-biased and, hence, dissipates power [58]. If the reverse bias exceeds the breakdown voltage, it irreversibly damages the shaded cell, assuming the module is not electrically protected [59–62]. Meyer and Dyk [26] have investigated the effect of reduced shunt resistance in shaded PV modules. In the partially shaded cell, the reverse breakdown in the localized region of the p-n junction results in the development of additional shunt paths across the junction, causing the overall shunt resistance to decrease. The study has reported a decrement in average shunt resistance in the cells ( $10.9 \Omega/\text{cell}$  to  $7.7 \Omega/\text{cell}$ ) under partial shading conditions.

### 2.4. Shunts due to temperature and humidity stress

The PV modules face temperature and humidity stress in the field, giving rise to a variety of defects [63–65]. However, the direct effects of temperature and humidity on the appearance of shunts, or on pre-existing shunts under field-aged PV modules, are not explored extensively. Sharma and Chandel [6] have reported localized increased recombination activity in cells of field-aged PV modules, similar to the shunting mechanism. Some studies have analyzed the effect of moisture on the leakage paths in solar cells [66–70]. In the field, moisture can penetrate a PV module from the laminated edges or the backsheet, resulting in increased leakage current in the cells [71]. This can be further increased as moisture also reduces the electrical resistance of the silicon material. Kim et al. [68] have observed an increase in the recombinative diode ideality factor ( $n_2$ ) under a damp heat test, indicating an increase in leakage current paths in the cells.

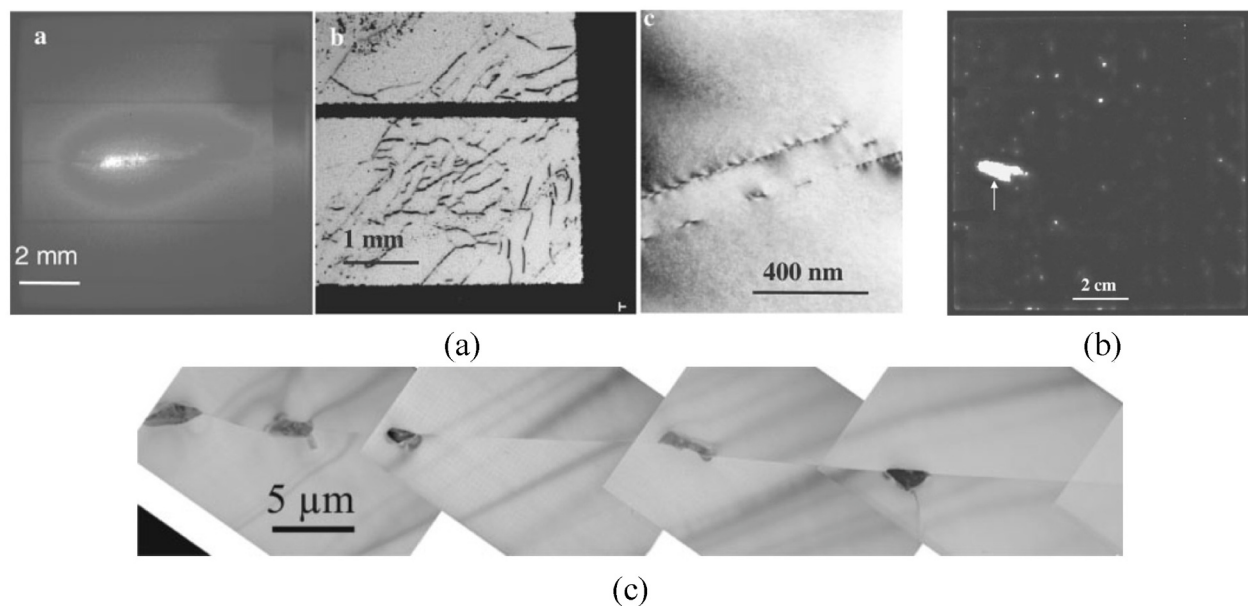


**Fig. 5.** Material induced shunts (a) shunt resulting from strongly recombinative crystal defects (b) shunt caused by  $\text{Si}_3\text{N}_4$  inclusion (c) shunt due to inversion layer at grain boundary [9].

### 2.5. Shunts due to potential induced degradation (PID)

PID-s has become one of the major problems in field-installed PV modules nowadays. It is a mechanism in which shunts are generated in the cells of the PV modules under high voltage stress [27,72–77]. Several studies have reported a reduction in shunt resistances under PID and an increase in the dark saturation current due to recombination in the space-charge region ( $J_{02}$ ) and the ideality factor ( $n_2$ ) of the recombinative diode term (two-diode model) [36,78], known as ohmic and non-ohmic PID respectively [79]. PID-s is associated with diffusion of metal ions, primarily sodium ( $\text{Na}^+$ ), from the front glass and encapsulation of the cell. These ions are driven into the silicon material by the existing high voltage [76]. The PID-s mechanism is shown in Fig. 6.

Several studies have observed that shunting activity under PID-affected modules is due to an increased concentration of  $\text{Na}^+$  ions in the cells. Specifically, some studies have reportedly investigated shunted regions at the micron and nanoscale through destructive testing on c-Si PV modules [31,32,34,37,80–82]. Harvey et al. [37] identified an

increased concentration (0.1 %–2 %) of  $\text{Na}^+$  ions at the  $\text{SiN}_x/\text{Si}$  interface, corresponding to structurally defected areas in the silicon itself. Naumann et al. [31,33,34] investigated the role of stacking faults in the formation of shunts during PID as shown in Fig. 7. The study identified that in faulty areas, more  $\text{Na}^+$  ions are likely to appear, resulting in shunting activity. PID-s is a reversible process, where the shunted regions can be recovered by diffusing away the  $\text{Na}^+$  ions however complete recovery is not possible in most cases [83–86]. Harvey et al. [37] reported a reverse shunting process under e-beam, where  $\text{Na}^+$  ions are diffused away to the surface from the shunted regions. This process is similar to the thermal recovery of the modules. The study also investigated a high concentration of oxygen at the defected locations; however, it does not play any role in shunt formation.

Table 1 provides a comprehensive overview of different types of shunts affecting PV cells, highlighting their origins, key characteristics, and impacts on cell performance. Edge shunts, arising from manufacturing processes and handling, are characterized by their presence along the edges of solar cells, contributing to reduced overall

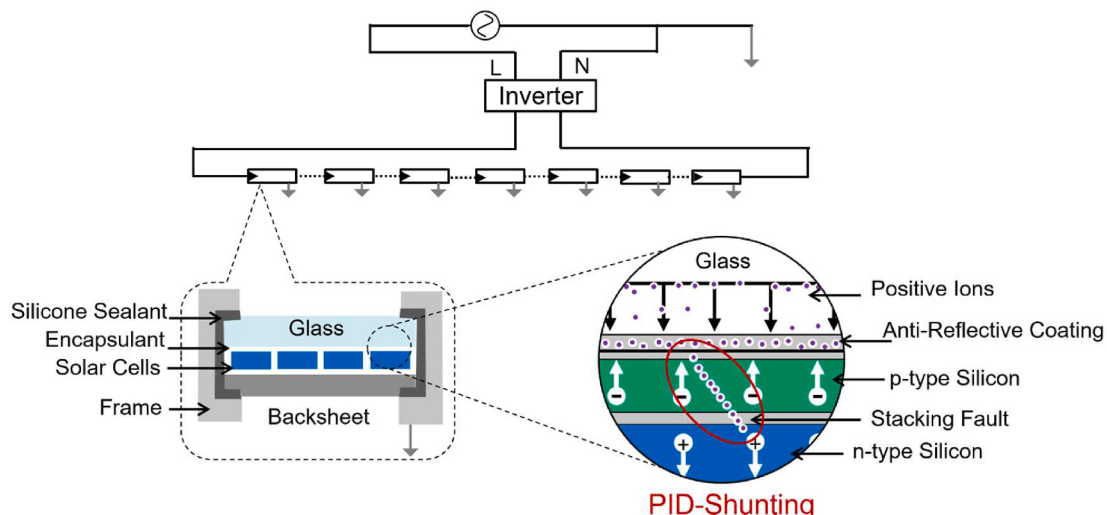


**Fig. 6.** Mechanism of PID-Shunting.

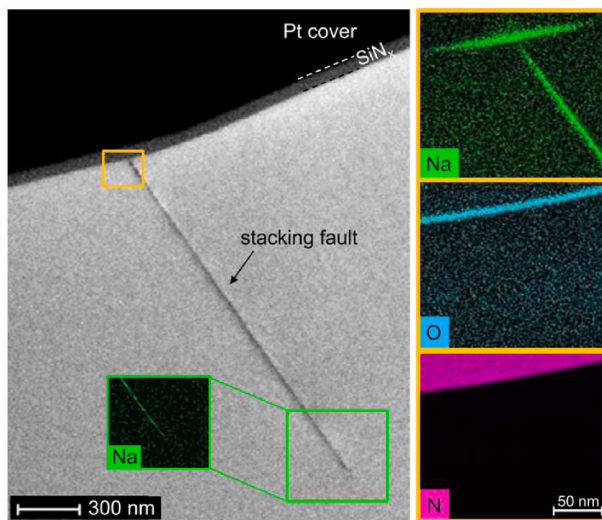


**Fig. 7.** TEM image with EDX mapping showing the presence of Na ions in the stacking fault [31].

efficiency and power output. Cracks and holes, resulting from mechanical stress and material defects, manifest as physical fractures and openings in the solar cell structure, causing increased leakage current and diminished electrical performance. The Schottky type shunt, originating from material impurities and junction issues, leads to the formation of a Schottky barrier at the metal-semiconductor junction, causing elevated dark current and decreased efficiency in low-light conditions. Other shunts, such as scratches, Al particle contamination, crystal defects, macroscopic SiN<sub>3</sub> inclusions, inversion layer at precipitates, shunt due to hotspots, shunt due to temperature and humidity, and potential-induced shunt, each present unique challenge and contribute to altered electrical properties, potential shunting, and decreased overall performance of PV cells under specific conditions. This comprehensive understanding of various shunt types is crucial for improving the design, manufacturing, and maintenance of solar cells to enhance their efficiency and longevity.

### 3. Detection and characterization of shunts

Detection and characterization are important for understanding the nature and characteristics of shunts, which can further aid in decision-making to minimize the shunting effect. The presence of shunts can be detected by observing the performance loss of the cells, and subsequently, the shunt can be spatially located using spatial characterization techniques. Characterization of shunts can be performed either destructively or non-destructively. Various characterization techniques are presented herein.

#### 3.1. Destructive characterization of shunts

Destructive characterization methods refer to the analysis of a specific cell/module region by physically extracting a sample from that cell/module. This is particularly relevant for detailed microscopic investigations in scanning and transmission electron microscopy (SEM and TEM), where specific shunt locations in solar cells can be studied. However, destructive characterization can only be performed after spatially locating the shunted region using spatial imaging techniques. Recently, some studies have been reported on the destructive characterization of shunts [9,17,87], aiming to understand the exact shunting mechanism.

Breitenstein et al. [9] utilized SEM and TEM for destructive characterization of the nature and origin of shunting problems in c-Si solar cells. Barbato et al. [11] performed SEM imaging of the hotspot region,

**Table 1**

Different types of shunts, their origin, key characteristics and impact on the PV cell performance.

Shunt Type	Origin	Key Characteristics	Impact on Performance
<b>Edge Shunt</b>	Manufacturing process, handling	Presence along the edges of solar cells	Reduced overall efficiency and power output
<b>Cracks and Holes</b>	Mechanical stress, material defects	Physical fractures and openings in the solar cell structure	Increased leakage current, reduced electrical performance
<b>Schottky Type Shunt</b>	Material impurities, junction issues	Formation of Schottky barrier at metal-semiconductor junction	Elevated dark current, decreased efficiency in low-light conditions
<b>Scratches</b>	Handling, abrasive contact	Surface marks or grooves on the solar cell	Reduced light absorption, potential for increased shunting
<b>Aluminum Particle</b>	Contamination during manufacturing	Presence of aluminum particles within the solar cell	Altered electrical properties, potential for increased shunting
<b>Crystal Defects</b>	Crystal growth issues, impurities	Structural anomalies within the semiconductor crystal lattice	Increased likelihood of shunting, reduced cell efficiency
<b>Macroscopic SiN<sub>3</sub> Inclusions</b>	Contamination during manufacturing	Large silicon nitride inclusions in the solar cell	Electrical isolation issues, potential shunting
<b>Inversion Layer at Precipitates</b>	Chemical reactions, impurities	Formation of inversion layers at precipitates in the material	Altered electrical properties, potential for increased shunting
<b>Shunt due to Hotspots</b>	Localized heating, uneven illumination	Hotspots leading to localized shunting	Reduced efficiency in affected areas, potential for cell damage
<b>Shunt due to Temperature and Humidity</b>	Environmental conditions	Sensitivity to temperature and humidity fluctuations	Increased risk of shunting and reduced performance
<b>Potential Induced Shunt</b>	Environmental factors, system issues	Formation due to potential differences in the solar cell	Increased leakage current, reduced overall system efficiency

which appeared after exploitation of a stress test, and identified the low-resistance signal path in the SEM image. Harvey et al. [37] introduced atom probe tomography (APT) analysis of PID shunting to understand the sodium content at the shunt-affected regions in the cells. They further extended their work by continuing to develop methods for multiscale, multi-technique characterization of PID shunting [81]. The study also investigated the role of oxygen in PID shunting using scanning TEM energy-dispersive X-ray spectroscopy (SEM-EDS) and TOF-SIMS 3D tomography.

Naumann et al. [29,31,32,34] utilized electron beam-induced current (EBIC) for the characterization of local shunts that appeared after PID stress tests. The study also used TEM imaging to observe the stacking faults responsible for PID. However, these types of characterizations are non-reversible, especially in the context of module integrity, as the module layers need to be detached in a destructive manner. Therefore, these types of characterizations have certain limitations, and more focus has been given to non-destructive characterization.

### 3.2. Non-destructive characterization of shunts

It is preferable to characterize shunts in PV modules through non-destructive means. Current methods for non-destructive shunt characterization fall into two main categories: spatially resolved and non-spatially resolved techniques [88–94].

#### 3.2.1. Non-spatial characterization techniques

The examination of the *I-V* characteristics in either forward or reverse bias is a widely employed non-spatial method, feasible for implementation in solar cells with readily accessible front and back contacts [93,94]. Both et al. [95] investigated the forward and reverse bias characteristics of localized shunts in c-Si solar cells and identified different shunt behaviors. However, this technique is unable to locate shunts in the first place without spatial imaging. Moreover, within modules, analyzing the *I-V* characteristics of shunts in individual cells poses challenges due to the influence of adjacent series-connected cells. Spatial characterization techniques offer a solution by imaging the entire or specific portions of the PV module, offering an effective means to pinpoint the precise locations of shunts within the cells.

#### 3.2.2. Spatial characterization techniques

Spatial techniques for shunt characterization are primarily divided into two categories: scanning-based techniques and camera-based imaging techniques. Carstensen et al. [88] developed an advanced Light Beam Induced Current (LBIC) measurement system called CELLO, employing a scanning-based approach to detect shunt locations in solar cells. Heide et al. [90] introduced another scanning-based system, Resistance Analysis by Mapping of Potential (RAMP), capable of shunt detection. However, both CELLO and RAMP techniques are time-consuming due to their scanning-based mechanisms. Balliff et al. [96] later introduced a quicker liquid crystal sheet method to localize shunts in silicon solar cells under reverse bias as shown in Fig. 8. While being cost-effective, these techniques are unable to differentiate between different types of shunts. Subsequently, the exploitation of advanced imaging techniques has enabled a more efficient understanding of the origin, nature, and severity of shunts.

**3.2.2.1. Detection of shunts by LIT.** Since shunts generate localized heat in solar cells, active Infrared (IR) thermography is effective for shunt detection. However, for precise shunt localization and increased signal strength, lock-in thermography is the most suitable technique [20,23, 98–100]. This technique utilizes the fluctuations in local temperature

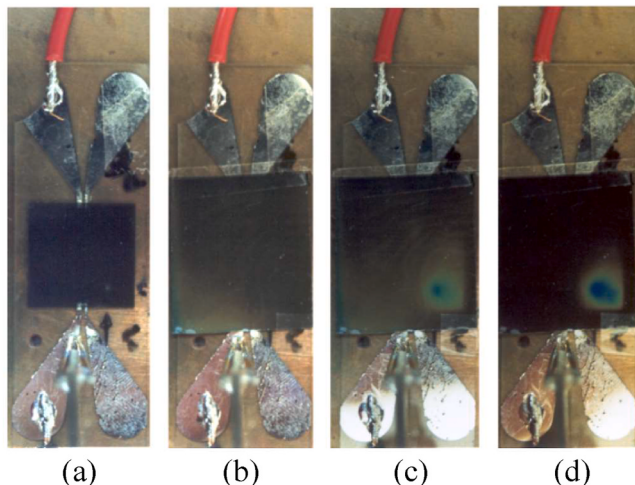


**Fig. 8.** Shunt localization on a thin-film solar cell (a) solar cell without cholesteric PDLC foil (b) solar cell covered with the foil without reverse-bias (c) with low reverse bias [97].

induced by shunt current when a pulsed bias is applied to the solar cell, to map out shunt locations [101]. The schematic of LIT setup is shown in Fig. 9.

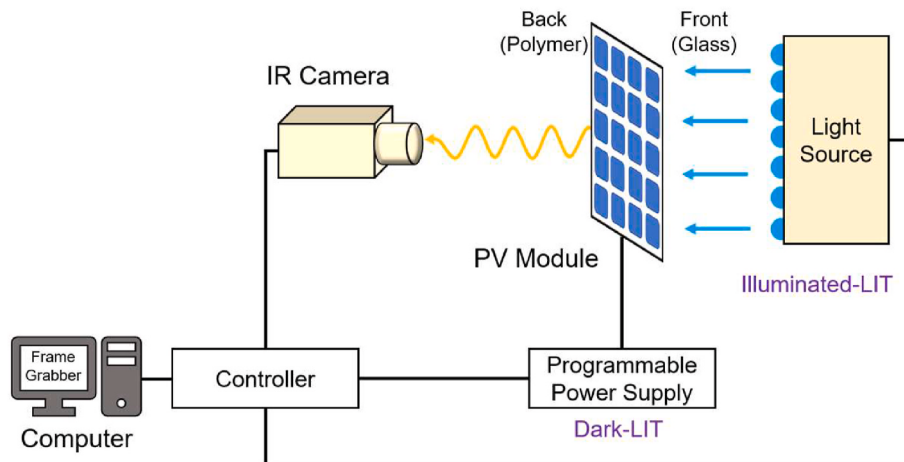
Several imaging studies utilizing the Dark Lock-in Thermography (DLIT) technique for shunt detection in solar cells have been presented in literature [41,87,99,100,102]. The technique demonstrates higher sensitivity for shunt detection; Breitenstein and Langenkamp [24] successfully detected shunts with currents as low as 100  $\mu$ A. Additionally, variation in the bias applied during DLIT enables the distinction between linear and non-linear shunts [17]. Linear shunts exhibit similar signal strength in DLIT images taken at both forward and reverse bias (close to the maximum power point of the cell), while non-linear shunts show a significant difference in signal strength. Some studies have successfully distinguished between linear and non-linear shunts in solar cells using this approach [103,104]. A sample investigation conducted by Gupta et al. [41] is shown in Fig. 10. If LIT is conducted using pulsed light irradiation under open circuit conditions ( $V_{oc}$ -ILIT), it can spatially image both the local lifetime inhomogeneities and shunts. In DLIT, under sufficiently small forward bias, the local lifetime variation does not significantly influence the signal, enabling only the detection of shunts [101,103].

While LIT is an efficient technique for application in single solar cells, the technique has some applicability constraints in modules. The low transmittance and low thermal diffusivity of the front glass in modules hinder effective characterization, impacting spatial resolution and the signal-to-noise ratio. Most of the studies have conducted DLIT from the Tedlar side of the modules. Roy and Gupta [43] effectively characterized shunts at different locations in the cells of the modules using DLIT in combination with Electroluminescence (EL). Also, distinction between linear and non-linear shunts is not possible using DLIT, in case of intact PV modules as reverse bias is not possible non-destructively.

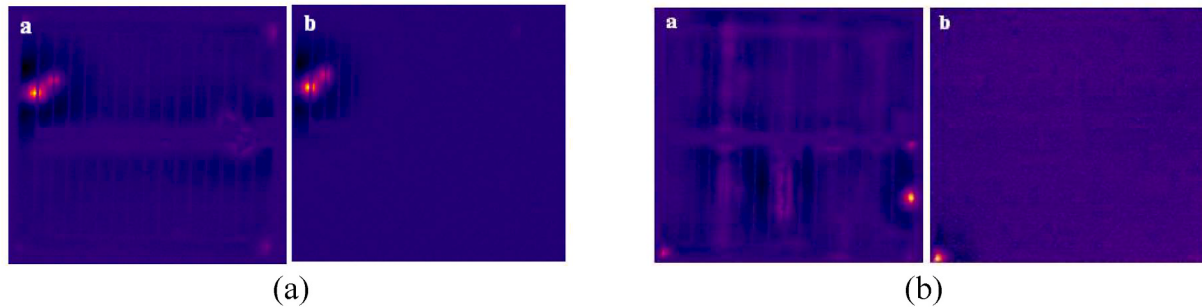
**3.2.2.2. Detection of shunts by luminescence imaging.** Imaging shunts in Electroluminescence (EL) and Photoluminescence (PL) is not as straightforward as in LIT. Breitenstein et al. [25] proposed an analogy with a distributed circuit network. During EL imaging, the externally supplied current to the cell spatially distributes via busbars and fingers and the recombination mechanism generates an EL signal. The schematic of EL is shown in Fig. 11 (a). Regions with low minority carrier density, i.e., defective regions, generate less EL signal, creating contrast with the good regions and making them detectable by the camera [105, 106]. However, the shunting mechanism differs. As shunts draw high localized current, they deplete current from their surroundings, creating a dark effect in the EL image [36]. This makes it challenging to distinguish shunts from other defects, particularly in large area module images. In PL (refer Fig. 11(b)), the shunt draws light-generated current, creating a darkness effect similar to EL, making it difficult to distinguish from other defects [107]. The depth and lateral extension of the dark region depend on the shunt resistance as well as the series resistance around it [108].

Fig. 12 represents the EL and PL images of cell parts in a module, where white encircled dark spots are localized shunts, as known from the DLIT image of the module. The utilization of EL and PL imaging for shunt characterization has been reported at a much later stage compared to LIT. Breitenstein et al. [25] reported that luminescence imaging allows identification of ohmic shunts only if they reach a certain limit. Many studies have compared shunt detectability in EL, PL, and LIT, concluding that shunt visibility is comparatively poor in EL/PL [109, 110].

Some studies have independently used Electroluminescence (EL) and PL imaging for shunt investigation. Abbott et al. [111] explored the appearance of shunts during a poor edge isolation process using PL imaging. Kasemann et al. [108] analyzed simulated luminescence images to locate and distinguish shunts from other defects. The study



**Fig. 9.** Schematic of lock-in thermography (LIT).



**Fig. 10.** DLIT images of (a) ohmic (linear) shunt (b) non-Ohmic (non-linear) Shunt [41].

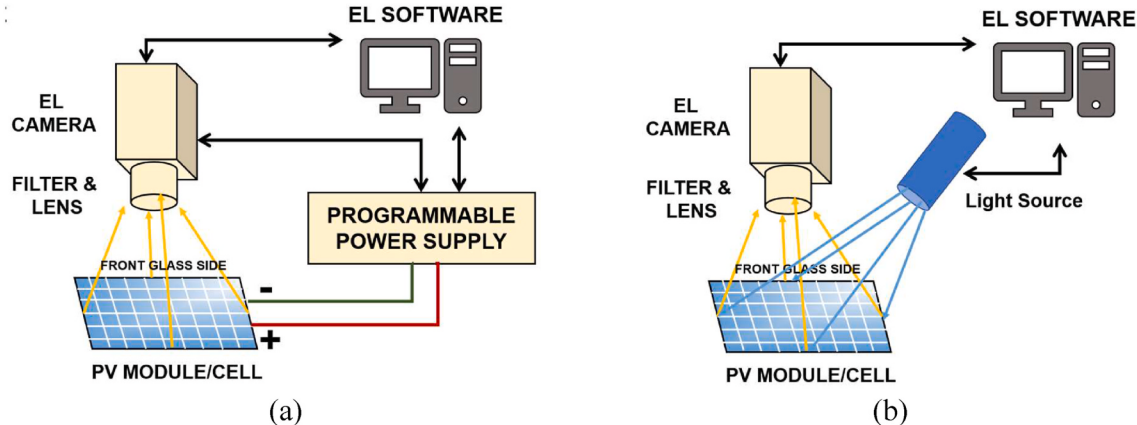


**Fig. 11.** Schematic of (a) electroluminescence (EL) imaging (b) photoluminescence (PL) imaging.

concluded that the images exhibit natural blurring at shunt locations, and shunt visibility is strongly dependent on the series resistance around it. Shunts under metallization are more likely to be identified. Sugimura et al. [112] distinguished non-linear shunts from other defects by performing reverse bias EL imaging. Breitenstein et al. [25] identified pre-breakdown sites in solar cells under reverse bias luminescence imaging. The study reported that not all pre-breakdown sites are visible in EL and PL, indicating a different electrical nature of these sites.

Some studies investigated the appearance of shunts in field-aged PV modules by EL imaging [113,114]. Many studies utilized EL imaging to observe shunting pattern recognition under PID stress [36,113,115]. The affected cells in the module appear darker at the edges with

diminishing darkness towards the center, and in the worst-case scenario, the cell becomes entirely dark. One sample PID-affected module is shown in Fig. 13. In the context of PID, some studies used DLIT to observe the exact shunt location in PID-stressed modules.

Roy and Gupta [43] employed a combination of Electroluminescence (EL) and DLIT for a qualitative understanding of shunt severity in c-Si PV modules. The study analyzed shunts at four different cell locations in a wide variety of manufacturer modules. DLIT was primarily utilized for detection, and various applications of EL imaging were exploited for this purpose.

### 3.2.2.3. Detection of shunts by fluorescent microthermal imaging.

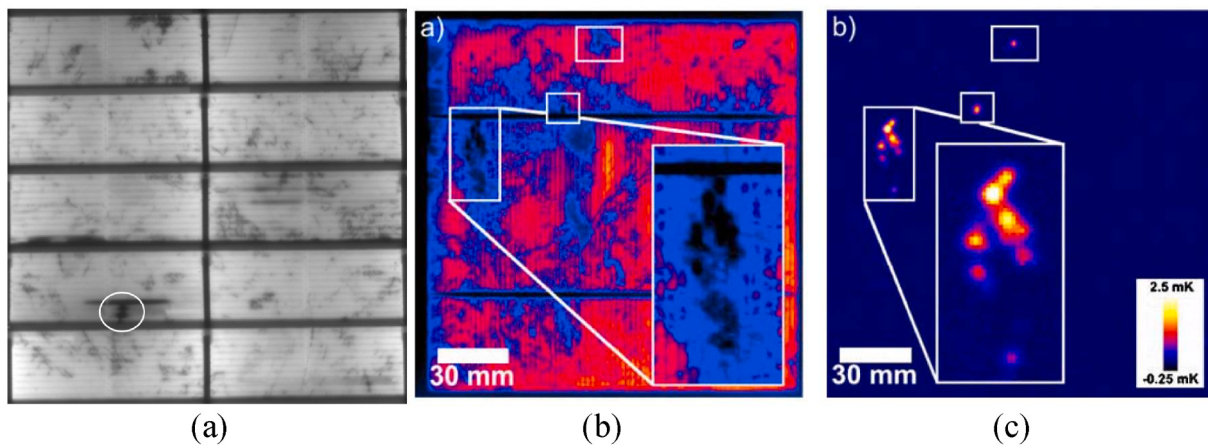


**Fig. 12.** Shunt investigation using (a) EL (encircled dark spots are shunts) (b) PL (in white rectangular box) (b) Cross verification using DLIT [25].

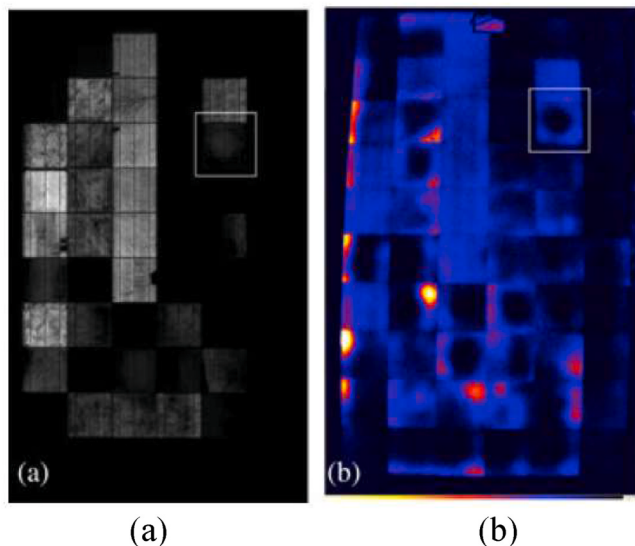


**Fig. 13.** (a) EL and (b) DLIT image of PID affected PV module.

Fluorescent Microthermal Imaging (FMI) leverages the temperature-dependent PL intensity of a luminescent thin film, often a polymer doped with rare-earth element-based luminescent species [116]. Spatial

data on absolute temperature variations in a sample are obtained by imaging the PL using a CCD camera. Local information regarding the sample's temperature evolution can be captured through a series of PL images. The basic experimental setup for FMI is straightforward, requiring an excitation source for PL, magnifying optics, and a CCD camera. Shunt detection, necessary for solar cell analysis, involves applying a bias voltage, requiring a voltage source. When coupled with an optical microscope, FMI can achieve high spatial resolution, approaching 0.3  $\mu\text{m}$ . This technique proves valuable in providing precise insights into the location of defects in solar cells. An energy diagram of the PL process is shown in Fig. 14 (a). The FMI setup is illustrated in Fig. 14 (b). The setup includes a UV source emitting at 365 nm to excite the PL in the luminescent thin film. A CCD camera is utilized to capture variations in PL intensity. FMI measurements involve the use of a simple power supply to apply a reverse bias. Fig. 14 (c) displays FMI images of a solar cell under 5 V reverse stress, illustrating the temporal evolution of temperature as a hotspot.

The described FMI technique is primarily limited to laboratory applications. This limitation arises from the necessity of coating samples with a luminescent thin film, followed by a specific heat treatment. These requirements place practical limitations on the quantity of samples that can be characterized. Additionally, the technique's utility diminishes for highly temperature-sensitive solar cells.

**3.2.2.4. Quantitative evaluation of shunts.** Some studies have undertaken quantitative evaluations of shunts to understand their severity,

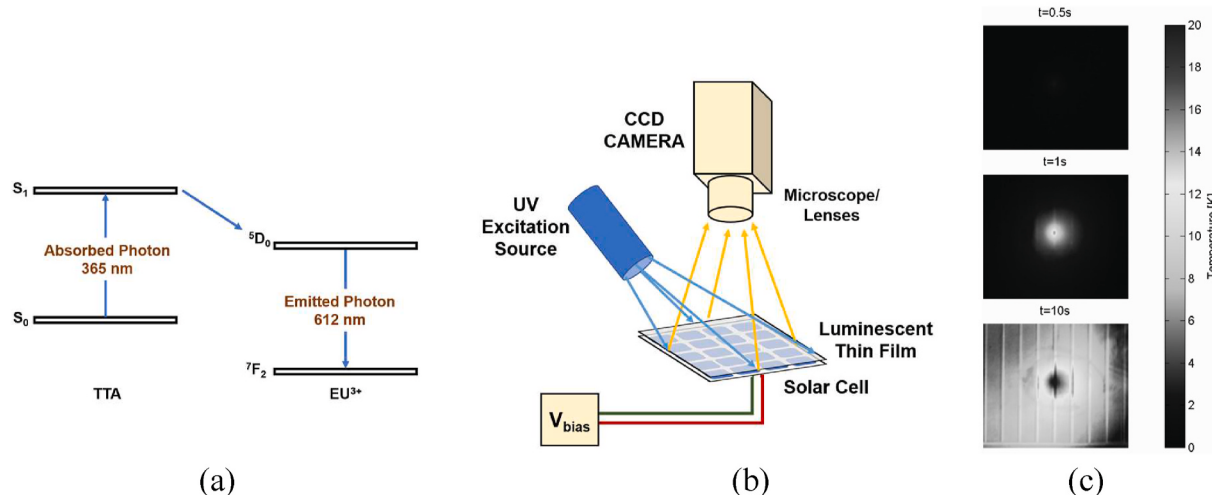


**Fig. 14.** Fluorescent microthermal imaging (a) PL energy diagram (b) setup (c) solar cell images [116].

correlate power loss, and establish priorities for shunt removal. Breitenstein et al. [117] utilized quantitative relations based on the lock-in principle and silicon material properties to estimate the current density of shunts. However, this process is complex and requires multiple executional steps. In comparison, luminescence techniques offer more advantages in directly correlating local voltage with luminescence intensity. Augarten et al. [118] used PL imaging to quantitatively estimate the current and voltage of ohmic shunts in solar cells and processed wafers based on the intensity drop, as depicted in Fig. 15. Nevertheless, as PL is highly sensitive to the uniformity and monochromaticity of the source light, the approach is not straightforward and demands significant precision.

Breitenstein et al. [22] utilized Electroluminescence (EL) imaging to quantitatively analyze localized shunts in solar cells. This method relies on quantitative relations in EL imaging to transform the EL image of a cell into a quantitative shunt image. However, it is only suitable for strong ohmic shunts and is susceptible to certain artifacts. Roy et al. [119] introduced an EL-based method for the estimation of shunt current and voltage in a single solar cell. Roy and Gupta [120] further extended their approach using EL into module scale and introduced a modified method for estimating shunt current and voltage in modules. Puranik et al. [36,113,115,121] attempted to correlate the power loss with the PID-s using QUEL and g-QUEL methods, with results shown in Fig. 16.

Building upon EL imaging, Kumar et al. [79] introduced a shunt index to non-destructively identify ohmic and non-ohmic shunts and assess their severity in a PV module, successfully overcoming the limitations of DLIT where forward and reverse biasing of the cell is necessary, which is not possible in an intact PV module. A PV module with shunt severity and nature is illustrated in Fig. 17. However, all these methods face several constraints for quantitative imaging in modules. As presented earlier, LIT does not have a straightforward application in modules. Additionally, the local potential in the module is floating, making it challenging for any quantitative interpretations. PL is challenging for application in modules due to constraints such as large-scale uniformity and interference of reflected light with the source. While EL fails in cases of severe shunting, as severely shunted cells do not produce any EL signal.

As an alternative to EL imaging for severely shunted cells, Kumar et al. [122] explored the possibility of using inverse IR thermography for quantitative shunt investigation. The PV cells in a module with varying severity were quantified, as shown in Fig. 18. Additionally, Kumar et al. [123] correlated the cell temperature with the power output of a shunted PV module based on a proposed model, as shown in Fig. 19 (a), and validation on 20 modules is presented in Fig. 19 (b).

**Table 2** compares various shunt characterization techniques, categorizing them based on their destructiveness, spatial capabilities, and advantages and disadvantages. Destructive techniques, such as SEM and TEM, offer high-resolution imaging but involve sample preparation and

are limited to surface details. Non-destructive methods, including IR Thermography and LIT, detect shunts without altering the sample, with IRT being non-contact and LIT having high sensitivity to local defects. However, IRT has limited spatial resolution, and LIT requires a controlled environment and may not be suitable for all materials. Electroluminescence (EL) Imaging maps internal defects with high contrast but is restricted to defects affecting carrier recombination. APT provides atomic-scale 3D imaging but has a complex operation and is limited to certain materials. EBIC maps carrier transport with high resolution but requires conductive samples and is limited to specific defects. Fluorescent Microthermal Imaging (FMI) provides temperature-dependent PL intensity, but its use is primarily limited to laboratory applications and necessitates coating samples with a luminescent thin film. Analysing *I-V* characteristics is non-destructive but struggles to locate shunts without spatial imaging, posing challenges in modules due to interference. The table offers insights into the trade-offs and considerations when choosing a shunt characterization technique for solar cells.

#### 4. Impact of shunts on performance and reliability

A localized shunt within a solar cell can draw excessive current, influencing both  $V_{oc}$  and FF, consequently decreasing  $P_{max}$ . Green [124] has deduced empirical relations to relate the loss in  $P_{max}$  and FF in the presence of shunt resistance. Even though the shunt resistance doesn't have much impact on  $I_{sc}$ , under severe conditions,  $I_{sc}$  may be affected. Loulou et al. [125] have shown the relationship between  $I_{sc}$  and shunt resistance of the solar cell. A variation in shunt resistance causes a mismatch in cells of the PV modules. Barbato et al. [126] have observed a significant variation in FF (~15 %) due to varying shunt resistances in newly manufactured sister solar cells. The study has analyzed that this variation is more prone to generating mismatch and hotspot formation in modules under field operations. Substantial power loss is attributed to shunts during periods of low irradiance, typically occurring in the morning and evening. Rummel and McMahon [127] have analyzed the effect of low irradiance on module performance in the presence of shunts. Pre-breakdown sites are localized regions in the solar cells that show low conductivity under low forward or reverse bias but exponentially increase at higher reverse bias (above -5 V typically) [57]. These sites do not contribute to the shunt resistance of the cell; however, they are potential contributors to hotspot generation under partial shading conditions. In the presence of pre-breakdown sites, mc-Si solar cells often start to breakdown between -5 and -15 V. These shunts are less harmful compared to ohmic shunts. However, they also degrade the FF and low irradiance performance of solar cells.

##### 4.1. Effect of shunts in modules

In the initial studies of solar cells, the shunt resistance was generally regarded as having a typical value. However, with increasing research on the performance of field-aged modules, it has been understood that the shunt resistance is dynamic and especially becomes severe under reduced light environments [127]. It has been observed that under prolonged exposure to light in the field, more shunt paths develop across the p-n junction of the solar cells. A decreasing shunt resistance reduces both  $P_{max}$  and FF of the modules. Especially in the absence of bypass diodes, the effect on modules becomes significant. The simulated *I-V* characteristics of a 36-cell c-Si PV module under the influence of decreased  $R_{sh}$  are shown in Fig. 20. A clear indication of a reduction in FF and  $P_{max}$  is observed in the curves.

Shunts are of major concern in the module aspect as they cause mismatches and may also lead to hotspot formation. If the shunted cell is partially shaded, it acts as a load for the entire PV module. At low shunt resistance, the shaded cell allows almost similar current flow through the shunt path as in the illuminated condition. This further increases the chance of hotspot formation and physical damage to the cell. If the shunt

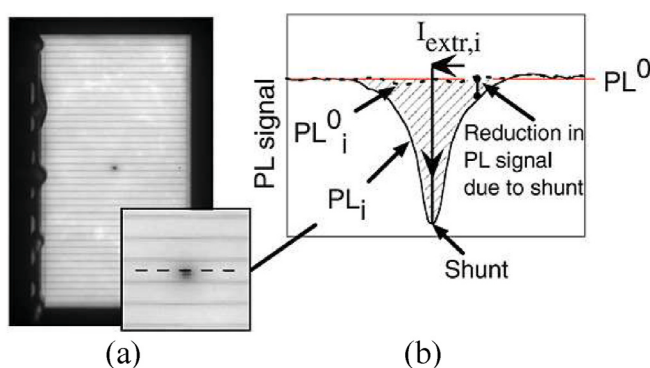


**Fig. 15.** (a) Photoluminescence (PL) image of a solar cell having a point-like shunt (b) Cross-section view of the PL signal across the shunt [118].

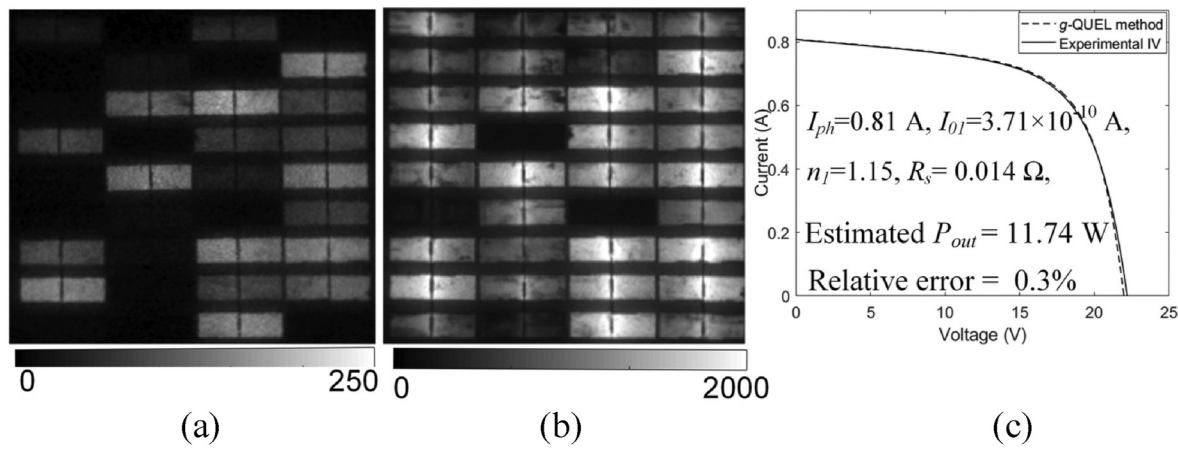


**Fig. 16.** EL image of a PV module (a) at low current (b) at high current (c) experimental and calculated  $I$ - $V$  characteristics [113].

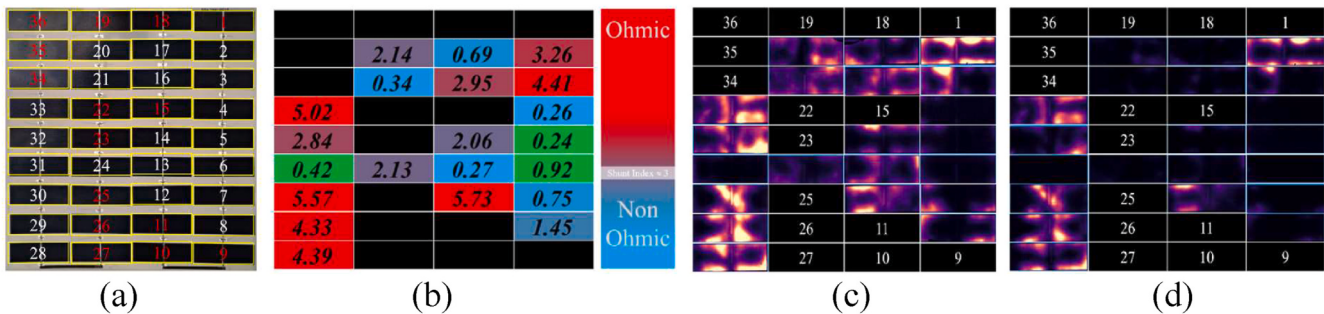


**Fig. 17.** (a) Visible image (b) cellwise shunt index values (c) forward DLIT (d) reverse DLIT images of PID-s PV module [79].

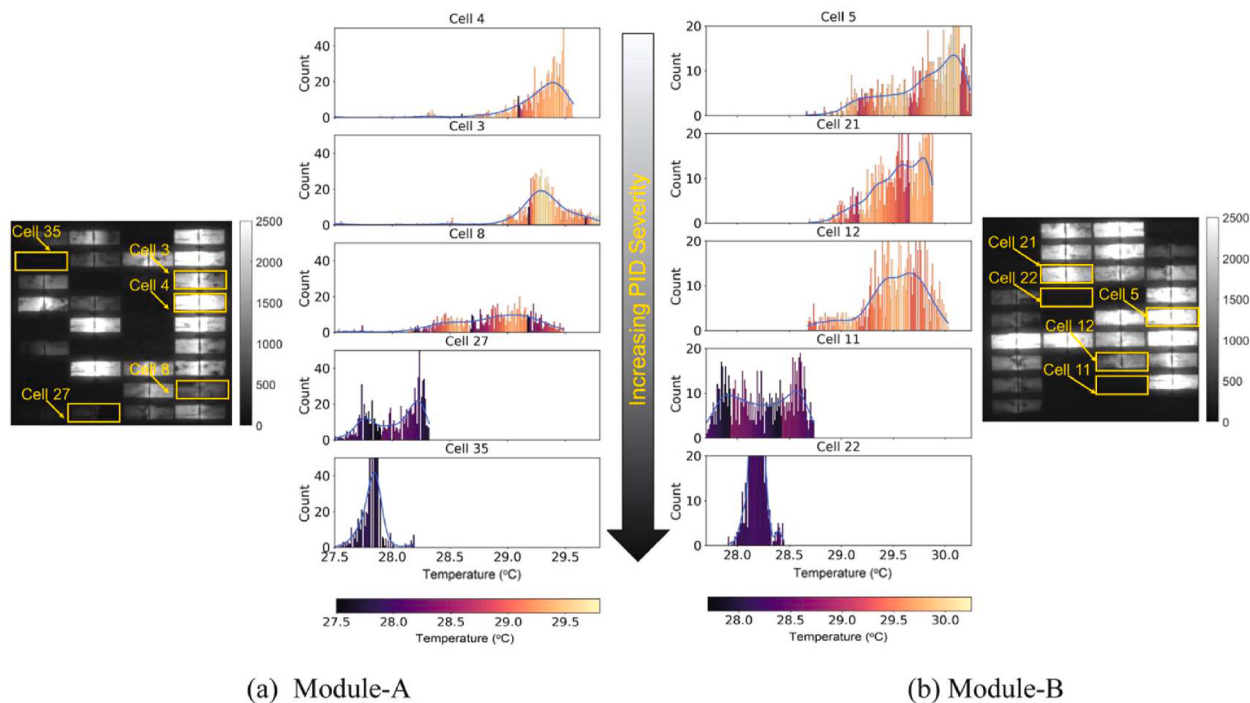


**Fig. 18.** PID-s cells based on shunt severity using  $\text{IR}_{\text{INV}}$  thermography [122].

resistance is low enough, a hotspot condition may occur even before the shaded cell enters the breakdown region [7,10,11,43,73]. Therefore, cells with lower shunt resistance have a higher chance of forming

hotspots, and subsequently, the cells forming hotspots are more likely to have low shunt resistance. With an increasing shading factor, the effect gets escalated [11]. Even if higher resistance shunt paths are burdened

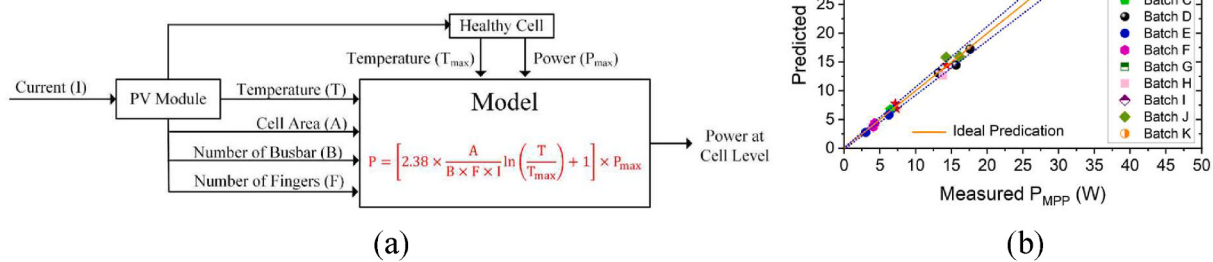


**Fig. 19.** (a) Proposed model to predict cell level power of PID-s cells (b) parity chart of power predicted using proposed model based on  $IR_{INV}$  thermography [123].

**Table 2**

Comparison of different shunt characterization techniques.

Technique	Destructive	Non-Destructive	Spatial	Non-Spatial	Advantages	Disadvantages
<b>Scanning Electron Microscopy (SEM)</b>	✓		✓		High-resolution imaging, surface analysis	Destructive sample preparation, limited to surface details
<b>Transmission Electron Microscopy (TEM)</b>	✓		✓		Atomic-scale imaging, internal structure	Highly destructive, complex sample preparation
<b>Infrared Thermography (IRT)</b>		✓	✓		Non-contact, detects thermal variations	Limited spatial resolution, surface-level information
<b>Lock-in Thermography (LIT)</b>		✓	✓		High sensitivity to local defects	Requires controlled environment, not suitable for all materials
<b>Electroluminescence (EL) Imaging</b>		✓	✓		Maps internal defects, high contrast	Limited to defects affecting carrier recombination
<b>Atom Probe Tomography (APT)</b>		✓	✓		Atomic-scale 3D imaging	Complex operation, limited to certain materials
<b>Electron Beam Induced Current (EBIC)</b>		✓	✓		Maps carrier transport, high resolution	Requires conductive samples, limited to certain defects
<b>Fluorescent Microthermal Imaging (FMI)</b>		✓	✓		Provides temperature-dependent PL intensity	Limited to laboratory applications, requires coating samples with luminescent thin film
<b>I-V Characteristics</b>		✓		✓	Analyses forward or reverse bias I-V characteristics	Unable to locate shunts without spatial imaging, challenging in modules due to interference

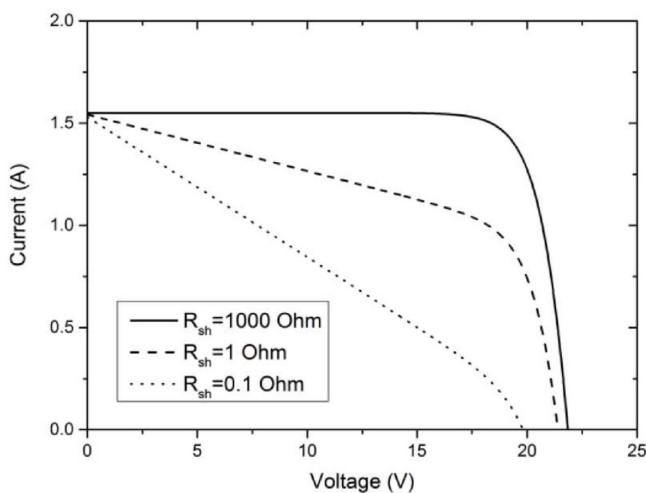


**Fig. 20.** Effect of decreasing  $R_{sh}$  on simulated I-V characteristics of a 36 cell c-Si PV module.

with a higher current level, they create additional localized temperature in the modules and enhance the chance of hotspot formation. Rossi et al. [128] have shown that the module current under shaded conditions strongly depends on shunt resistance. Lower shunt resistance results in

more power dissipation through the cell. This power dissipation can lead to a notable rise in temperature in regions of the PV cell near impurity centers, resulting in hotspot heating. Barbato et al. [11] have carried out stress tests to characterize the dynamics of the degradation process under partial shading conditions and physically observed localized hotspot formation in the cells of the modules as shown in Fig. 21. The study has reported power dissipation on the order of tens of watts at the shunted location.

#### 4.2. Modeling and simulation of shunts

Understanding the exclusive impact of a shunt within a module poses a challenge. In field-aged modules, there are different sources of degradation, making it challenging to assess the effect of the shunt alone. For the purpose of assessing the effect of shunts, modeling and simulation are the most convenient and well-reported approaches. The 1-diode and 2-diode modeling of solar cells (lumped models) is the most fundamental and easy-to-implement approach for the study of shunts [15,38,129–131]. Among these, the 2-diode model has been used extensively. The 2-diode model, also known as the double diode model (DDM), is depicted in Fig. 22(a) and (b), with the impact region on the curve shown in Fig. 22(c). Many literature has used these approaches to understand the effect of shunt resistances in solar cells [15,130]. Dyk and Meyer [132] examined the impact of ohmic shunt resistance on PV module performance through simulation (PVSIM), replicating the ohmic shunting effect in a 36-cell c-Si PV module. The research indicated that

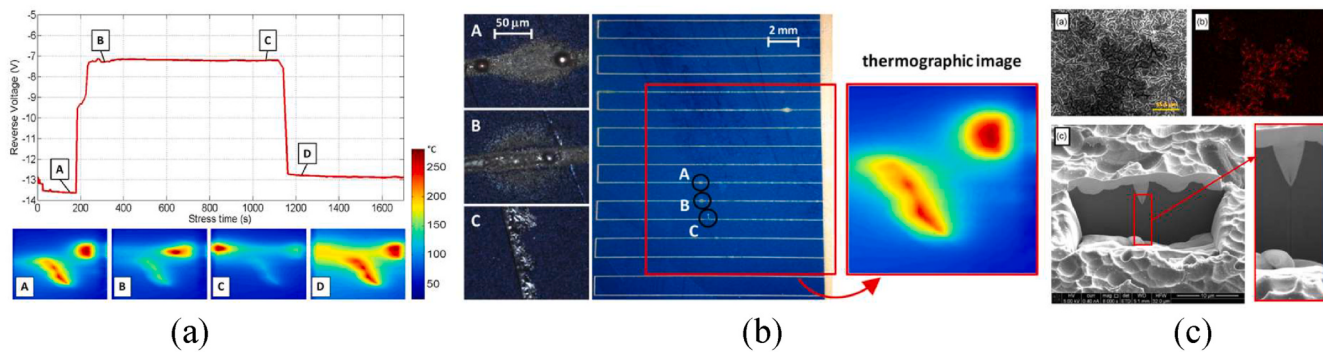


**Fig. 21.** Hotspot formation due to partial shading on a shunted cell in a PV module (a) Reverse voltage across the cell with time (b) Microscopic image of the induced hotspots (c) SEM images of shunted sites [11].

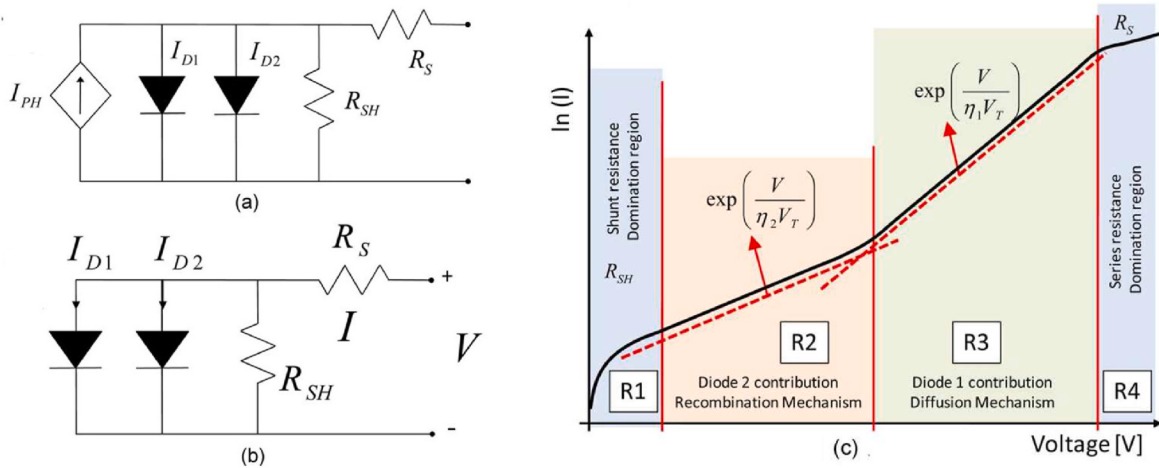


**Fig. 22.** (a) DDM under illuminated conditions (b) DDM under dark conditions (c) Contribution of each diode and resistance on the dark  $I$ - $V$  characteristics [11].

the slope of the reverse  $I$ - $V$  characteristic undergoes significant alterations with decreasing shunt resistance ( $R_{sh}$ ). Dhass et al. [10] employed MATLAB to simulate shunt resistance in a solar cell and observed a notable enhancement in the fill factor (FF) of the cell (from 0.3 to 0.8) by increasing shunt resistance (from  $1 \Omega$  to  $10 \Omega$ ). Furthermore, it was noted that the modules containing cells with low  $R_{sh}$  experience a rapid decline in efficiency under reduced irradiance levels.

#### 4.2.1. Distributed electrical modeling

The lumped models are capable only for understanding the shunt effects in a global scenario. These approaches cannot incorporate the spatial variation due to localized shunts in solar cells. To understand the spatial shunt effects in the presence of metallization and varying current flow in the cells, distributed models are more suitable. The electrically distributed analysis proves beneficial for comprehending cell performance across different shunt parameters. It could serve in categorizing

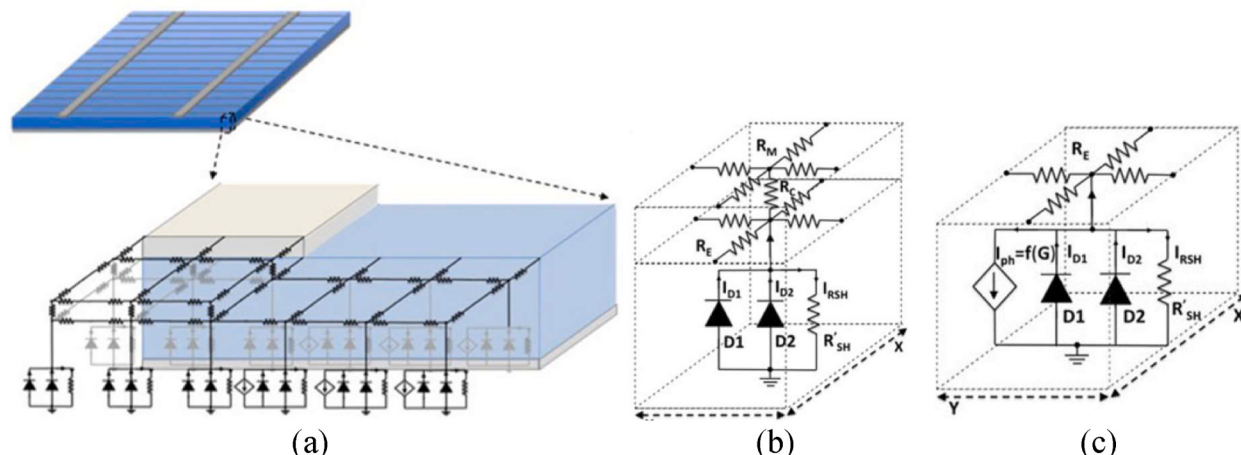


**Fig. 23.** (a) Distributed diode model of a PV cell (b) Elementary unit based on the two-diode circuits for metalized area (c) Elementary unit for non-metalized area i. under the busbars and fingers [134].

shunts into various classifications based on tolerance levels, facilitating prioritization in addressing shunting issues. Zekry and Al-Mazroo [133] introduced a Spice-based distributed diode modeling approach to the solar cell, in which the location-specific effect of shunts can be modelled as shown in Fig. 23.

Several simulation studies have shown the spatial effect of shunts on cell and module performance by distributed diode modeling using PSpice simulation software [35,40,135]. Gupta et al. [41] have reported power loss due to shunts ranging from 3 to 15 % in mc-Si solar cells and found that shunts under busbars are most severe compared to those at the edges. This occurs because the shunt positioned beneath the busbar draws current from the busbar with lower resistance, contrasting with the higher-resistance emitter in cases of shunts located at the edge. Roy and Gupta [43] employed a simulation method to identify spatial variations in severity resulting from shunts located at various positions within the cells (edge, corner, under finger, and busbar). The study also shows that shunts under metallization, specifically under busbars, are most severe. Somasundaran and Gupta [40] conducted an analysis of the alteration in the *I-V* characteristics of solar cells under the influence of changing shunt resistances, proximity to metallization, varying shunt area, and different irradiance levels. The research also determined that performance is significantly influenced by the shunt's position and its closeness to metallization. Notably, the study observed relative power losses of up to 80 % under low irradiance conditions. It is found that for a similar absolute shunt resistance value, the shunt having a higher area is more degrading, considering the proximity to metallization. Additionally, it has been observed that sheet resistivity plays a crucial role in the shunting effect. Higher sheet resistance results in enhanced shunt screening, consequently improving performance in the presence of shunts. Moreover, sheet resistivity has a greater impact on shunts not under metallization, as the current conducted by the shunt traverses through the emitter layer. Another study by Somasundaran and Gupta [12] has quantitatively investigated the possible improvement in efficiency and FF of solar cells by avoiding shunt formation at particular cell locations (metallization/non-metallization) under corrective measures taken at cell production.

Table 3 presents various electrical modeling approaches for shunt

**Table 3**  
Different modeling approaches for shunt simulation studies.

Model	Type	Capabilities	Accuracy	Suitability
<b>Single Diode Model</b>	Electrical	Basic representation of a solar cell's electrical behavior. It considers one diode for the main p-n junction.	Moderate accuracy for simple systems	Suitable for quick simulations and initial assessments
<b>Double Diode Model</b>	Electrical	More sophisticated than the single diode model, incorporating two diodes to account for additional losses and complexities.	Improved accuracy for diverse systems	Suitable for a more detailed analysis of solar cell behavior
<b>Distributed Diode Model</b>	Electrical	Represents a solar cell with multiple diodes distributed across its area, capturing spatial variations in electrical properties.	High accuracy, especially for spatially varying characteristics	Suitable for detailed simulations of complex solar cell structures and shunting effects

simulation studies, each catering to different levels of complexity and accuracy in representing solar cell behavior. This table can be used to choose the most appropriate modeling approach based on the desired level of detail and accuracy for their specific shunt simulation studies.

#### 4.2.2. Thermal modeling

The operational temperature of the module significantly impacts its performance. Numerous research studies have explored how changes in module temperature affect the performance of modules deployed in real-world conditions [59,70,123,135–142]. The literature on the distributed diode model mentioned earlier does not consider the thermal effects due to the temperature rise at the shunted location in the module. During field operations, the shunted area generates heat, which disperses across various layers of the module, leading to mismatch and performance loss due to elevated operating temperatures. This effect is get escalated under partial shading conditions, where the shunted area generates even more heat. In this context, Somasundaran et al. [135] have proposed a thermal model (refer Fig. 24) of the PV module to estimate mismatch losses attributed to shunts, taking into account heat distribution across various layers of the PV module. A comparison between electrical and thermal parameters is provided in Table 4. The research demonstrated the performance degradation resulting from mismatch induced by shunts across varying numbers of shunted cells.

## 5. Prevention and mitigation of shunts

This section describes few prevention and mitigation techniques for shunt at fabrication stage, operation stage and later correction stage.

### 5.1. Prevention at fabrication stage

In order to minimize shunts, the first possible step is to improve certain fabrication techniques at the cell manufacturing stage. It was found that poor edge isolation and non-optimized contact firing are the most common process-induced faults responsible for shunt formation [9, 17,42,143]. Some studies have presented different advanced processes of edge isolation to avoid defects arising from this technique. Several improved and alternative techniques such as laser-doped techniques, waterjet-guided lasers etc. have been introduced for a better edge isolation technique. Hauser et al. [144] have performed a comparative study of different methods for edge isolation techniques. The study used *I-V* analysis, LBIC, and LIT to investigate the possible shunt formation for these different techniques in solar cells. Haupt et al. [145] introduced an enhanced laser edge isolation technique for c-Si solar cells employing a high-power picosecond laser. Chithambaranadhan et al. [146] introduced a chemical etching process to repair shunts formed due to a faulty screen-printing process, cracks filled with Ag and Al particles, etc. However, the process is complicated and needs simplification for commercial implementation.

### 5.2. Role of bypass diode

In shunted cells, the effect could be minimized either by diverting the cell or by physically isolating the shunted region. Generally, under partial shading conditions, the bypass diode itself takes care of the reduced performance of the shunted cell [147,148]. In partial shading conditions, the shaded cell itself generates less current than its neighboring cells and reduces the string current in the absence of bypass diodes. However, if the cell is shunted, most of the current flows through the shunt, which maintains a higher current flow in the string. It increases the chance to generate localized heat and thus a hotspot [149, 150]. However, if the shunt has a larger area, or the recombination effect is distributed, then there is less probability of generating a hotspot. However, the effect of the shunt on the string current under partial shading conditions has not been explored much, and thus no concrete conclusions can be drawn.

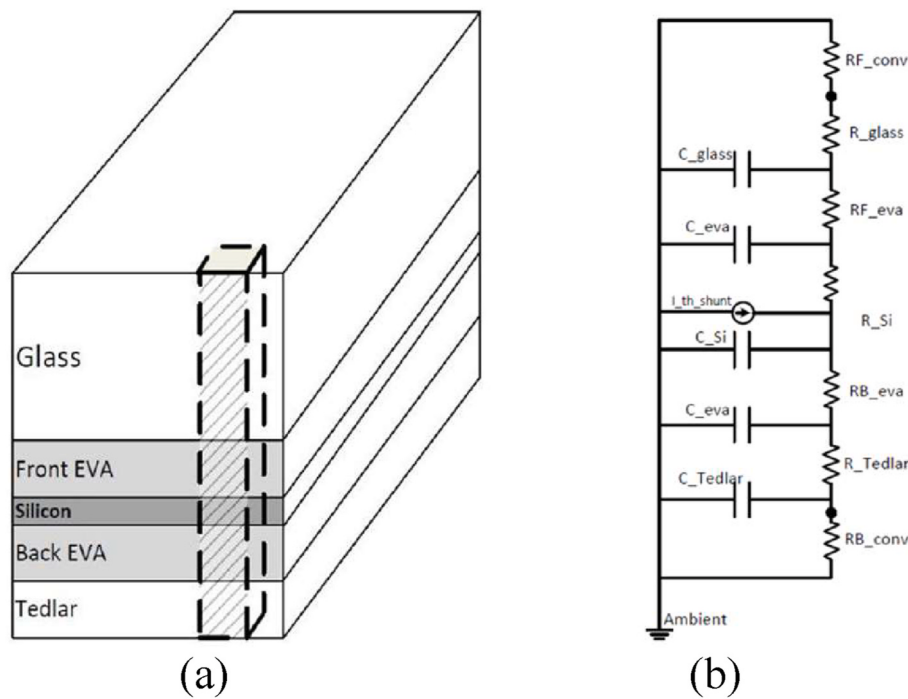


**Fig. 24.** (a) Cross-sectional view of solar cell (b) Electrical equivalence of thermal model [135].

**Table 4**  
Analogy between electrical and thermal quantities.

Equations	Analogy
$I = \frac{\Delta V}{R_e}; q = \frac{\Delta T}{R_f}; R_t = \frac{l}{kA}$	$V \leftrightarrow T; R_e \leftrightarrow R_f; I \leftrightarrow q$
$I = C \frac{dV}{dt}; q = mc_p \frac{dT}{dt}$	$C \leftrightarrow mc_p$

### 5.3. Approaches for preventing PID-s

PID-s in a PV module can be prevented at three levels i.e., system level, module level and cell level. At system level, high negative bias of cells in a PV module need to be avoided by grounding the negative terminal of the string or by using other means involving micro/mini inverters [27]. At module level, first of all the amount of  $\text{Na}^+$  need to be minimized by using quartz glass or other glass having less mobile ions as a front glass. Also, encapsulants with reduced ions mobility can be

utilized to prevent the drift of  $\text{Na}^+$  from the front glass to the cell surface [66]. At cell level, to prevent the drift of ions across the  $\text{SiN}_x$  layer can be prevent by lowering the potential across  $\text{SiN}_x$  layer through increased conductivity by increasing the refractive index or doping. Also, modification in Si surface before  $\text{SiN}_x$  deposition can also help in preventing PID-s in a PV module [151].

### 5.4. Physical and chemical isolation

For physical removal, the generally reported process for shunt isolation is to locate the shunted region by means of spatial imaging, followed by a combination of laser ablation and wet chemical etching of silver contact fingers to minimize the shunting effect [146]. Several studies introduced laser isolation techniques for the physical isolation of the shunted region. Abbott et al. [111] used Nd:YAG laser to isolate localized shunts in an industrial c-Si solar cell and observed a significant improvement in efficiency (9.6 %–13.3 %) as shown in Fig. 25.

Similarly, Augarten et al. [152] performed laser isolation in multiple

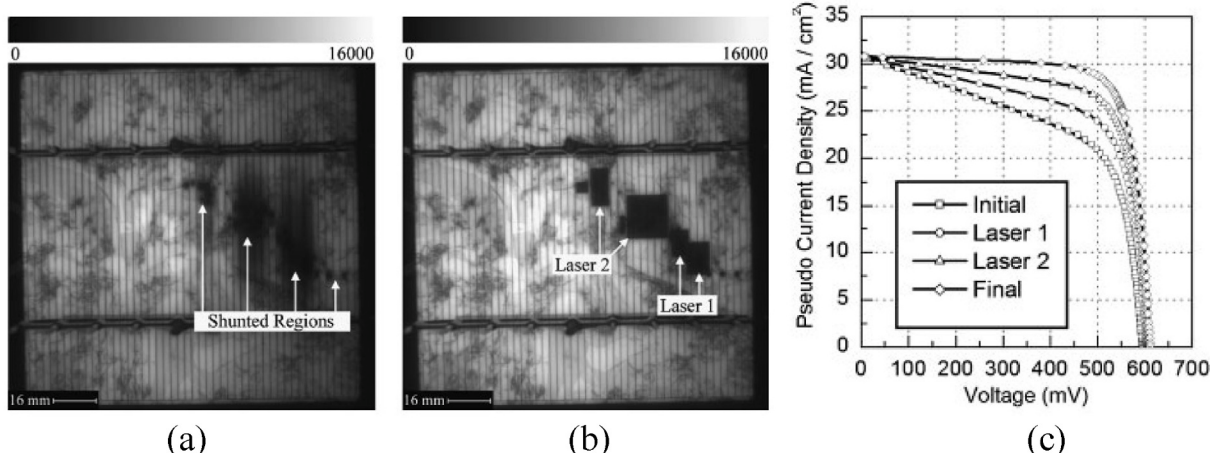


**Fig. 25.** PL images (a) before and (b) after laser isolation (c) I-V characteristics of laser treated PV cell [111].

solar cells, which were rejected due to failing to meet the standard criteria, and observed a significant increase in efficiency and FF that enabled the cells to be reused considering industrial standards as shown in Fig. 26.

Hao et al. [153] combinedly exploited laser scribing and chemical etching to optimize the isolation effect and reported a significant improvement in the cell characteristics as shown in Fig. 27.

Zhang et al. [154] physically isolated shunts at the edges and replaced the isolated region with a good cell part by connecting parallelly. It significantly improved the  $I_{sc}$  of the cell (3.71–4.11 A) that enabled the cell to be reused for module formation as shown in Fig. 28.

The presented shunt removal techniques are more of manual implementation rather than in-line application. Therefore, more focus and precautions should be given to the initial fabrication stages.

**Table 5** offers a comprehensive comparison of various preventive and mitigation techniques employed in the context of shunting in PV systems. The techniques are assessed based on efficiency improvement, applicability to different PV technologies, and associated challenges. This table serves as a valuable resource for decision-making, allowing stakeholders to weigh the pros and cons of each technique based on their specific efficiency improvement goals, technology preferences, and risk tolerance.

## 6. Discussion and future scope

Shunts, recognized as severe defects and sources of degradation, have a long history in crystalline silicon PV modules. Fig. 29 summarizes the types of shunts, their characterization, modeling approaches, and mitigation techniques. The impact of shunt resistance on the degradation of crystalline silicon PV modules presents several critical challenges that need to be addressed to improve the performance and longevity of solar energy systems. This review highlights the following key issues.

● **Historical Context and Evolution of Shunts:** Initially, process and material-induced shunts were prevalent due to rudimentary fabrication processes. Over time, shunts arising from hotspots, shading, temperature, humidity, and potential stress have emerged. Process-induced shunts result from manufacturing processes involving contamination, defects, or other process variations, while shunts occurring during operation develop over time. Although, advances in instrumentation and fabrication processes have substantially reduced process-induced shunts, and material processing improvements have minimized shunts caused by material dislocations.

○ **Main Issue:** However, new shunts related to external factors like hotspots, shading, temperature, humidity, and potential stress continue to emerge. Sometimes, weak process or material-induced shunts, undetected during fabrication, may intensify into strong shunts under reverse voltage stress during partial shading.

Therefore, quality control and maintenance are crucial for addressing shunt-related challenges in PV systems.

○ **Follow-up Research:** Focus on improving quality control during fabrication and developing advanced materials that resist new forms of shunt-related degradation is required. Additionally, real-time monitoring systems should be explored to detect and mitigate emerging shunt types in operational PV modules.

● **Characterization Techniques:** Different characterization techniques reported for analysing shunts have distinct advantages and disadvantages. SEM and TEM offer high-resolution imaging but require destructive sample preparation. IR thermography and LIT provide non-contact detection of defects but may lack spatial resolution. EL imaging maps internal defects with high contrast but is limited to defects affecting carrier recombination. APT and EBIC offer atomic-scale imaging and carrier transport mapping but are operationally complex. FMI provides temperature-dependent photoluminescence intensity but is mainly applicable in laboratory settings. For encapsulated PV modules, non-destructive spatial imaging technique such as LIT and EL are useful for gaining insights into defects or degradation. However, destructive techniques such as SEM and TEM are utilized for understanding the origins of shunts at atomic level. Recently, non-destructive methods, including scanning-based and camera-based imaging techniques, have used for early-stage detection and shunt's impact quantification on solar cell performance.

○ **Main Issue:** Each characterization technique for shunts, such as SEM, TEM, IR thermography, and EL imaging, offers distinct advantages and limitations. While some techniques provide high-resolution imaging, they often require destructive sample preparation, limiting their application in a practical setting.

○ **Follow-up Research:** Research should prioritize the development of non-destructive, high-resolution imaging techniques that can be effectively used in real-world conditions. Additionally, combining various techniques could provide a more comprehensive understanding of shunt defects, that need to be explored.

● **Modeling Approaches:** Various models are used for solar cell analysis, each offering different capabilities and levels of accuracy. The Single Diode Model provides a basic representation of electrical behavior suitable for quick simulations. The Double Diode Model incorporates additional losses and complexities for improved accuracy. The Distributed Diode Model captures spatial variations in electrical properties, offering high accuracy for detailed simulations of complex solar cell structures.

○ **Main Issue:** Existing models like the Single Diode Model, Double Diode Model, and Distributed Diode Model each offer varying levels of accuracy and complexity in representing solar cell behavior under the influence of shunts. However, these

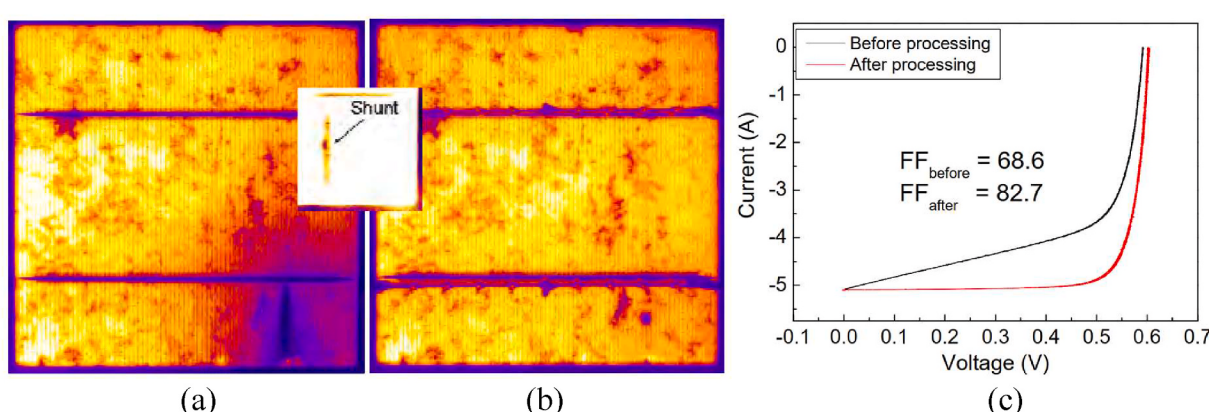


**Fig. 26.** PL image of a strongly shunted cell (a) before shunt isolation, (b) after isolation (c) I-V characteristics of shunted cell before and after shunt isolation [152].

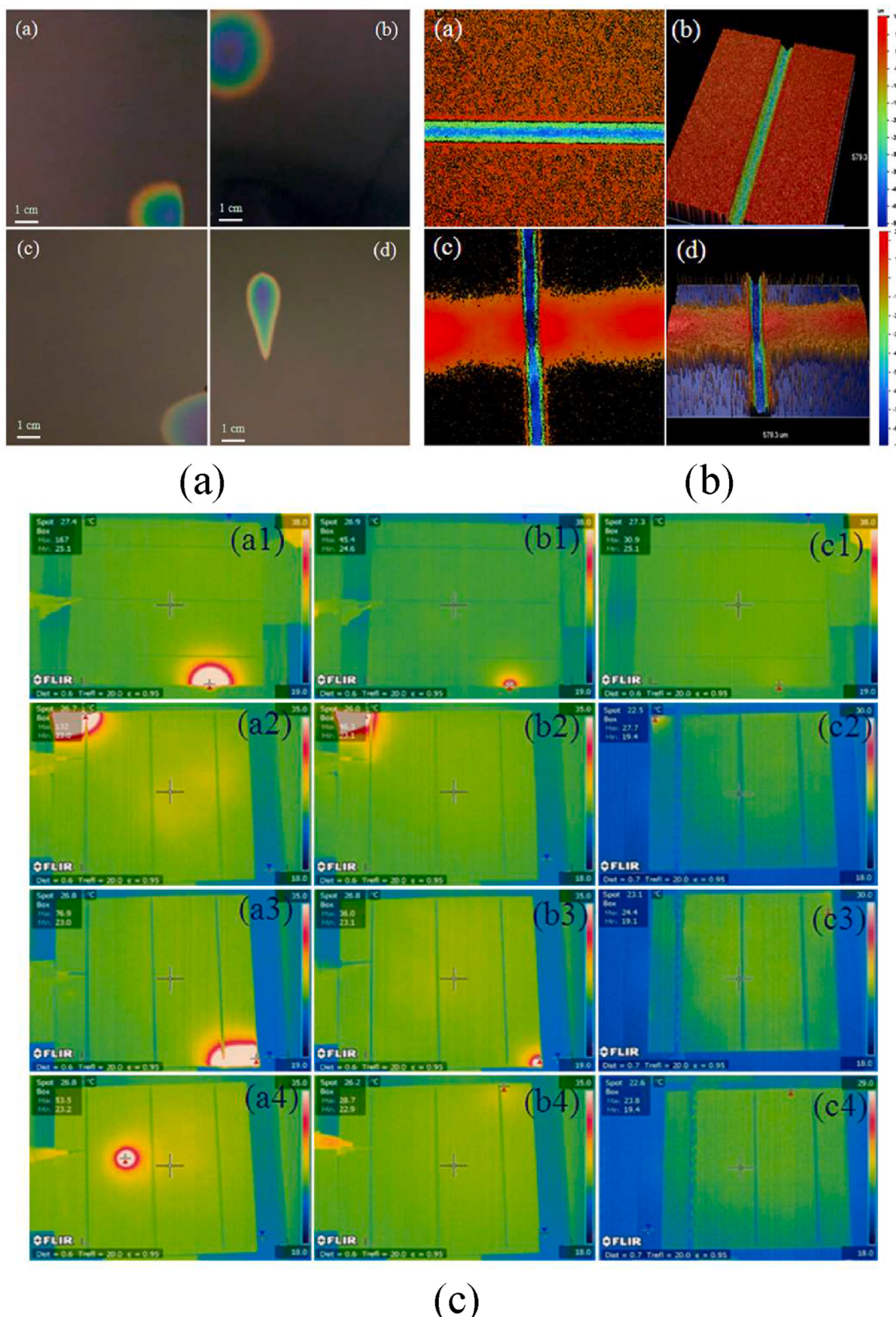


**Fig. 27.** Isolation of shunts in silicon solar cells through a combination of laser and chemical etching processes (a) shunt location (b) laser isolation (c) results initial and after laser isolation and chemical etching [153].

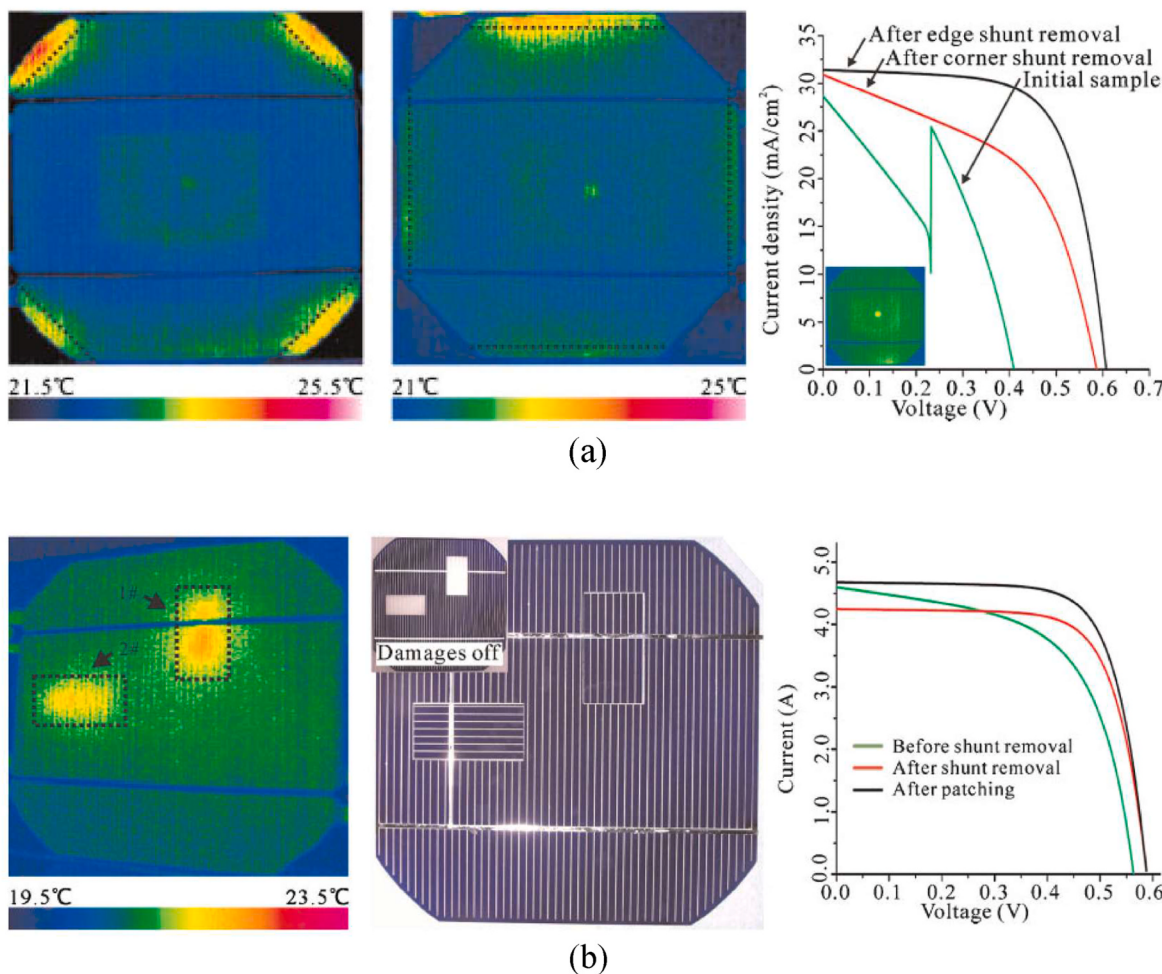


**Fig. 28.** Elimination and patching of shunts in c-Si solar cells through IR imaging and laser cutting [154].

**Table 5**

Comparison of various preventive and mitigation techniques.

Technique	Efficiency Improvement	Applicability to Various PV technologies	Challenges
<b>Physical Removal/Isolation</b>	Depends on the extent of shunting removed	Broad, applicable to various PV technologies	Labor-intensive, may damage the solar cell during removal
<b>Bypass Diode</b>	Mitigates losses in shaded or shunted areas	Commonly used in various PV technologies	Limited effectiveness for widespread shunting issues
<b>Advanced Edge Isolation</b>	Reduces edge-related shunting	Applicable to different PV technologies	Increased manufacturing complexity, potential cost
<b>Chemical Etching</b>	Improves surface properties, reduces shunting	Applicable to crystalline silicon PV	Environmental concerns, selective etching challenges
<b>PID-s Prevention</b>	Prevents potential-induced degradation at the system level	Suitable for various PV technologies	Requires careful system design and monitoring
<b>Module Level</b>	Mitigates potential-induced degradation at the module level	Applicable to different PV technologies	Module-level implementation may not address all issues
<b>Cell Level</b>	Addresses potential-induced degradation at the cell level	Commonly applied in various PV technologies	Limited to addressing specific PID-s related challenges
<b>PID-s Mitigation</b>	Mitigates potential-induced degradation effects	Applicable to various PV technologies	Requires additional components, potential cost increase

models often require a trade-off between accuracy and computational efficiency.

o **Follow-up Research:** Future research should aim at developing advanced simulation tools that can accurately capture the dynamic nature of shunts, especially in field-aged PV modules. Emphasis should be on improving computational efficiency without compromising accuracy.

● **Mitigation Strategies:** The type of shunt determines the appropriate mitigation strategy. Pointed shunts induced by processes or materials can be physically removed, while bypass diodes are effective for preventing mismatches between cells, avoiding hotspots and shunting in PV modules. Initially, physical and chemical isolation were used to remove the shunted region developed during fabrication in a PV cell. For mitigation and prevention in the field, bypass diodes are commonly used as a safety mechanism. PID-s generally spread over a

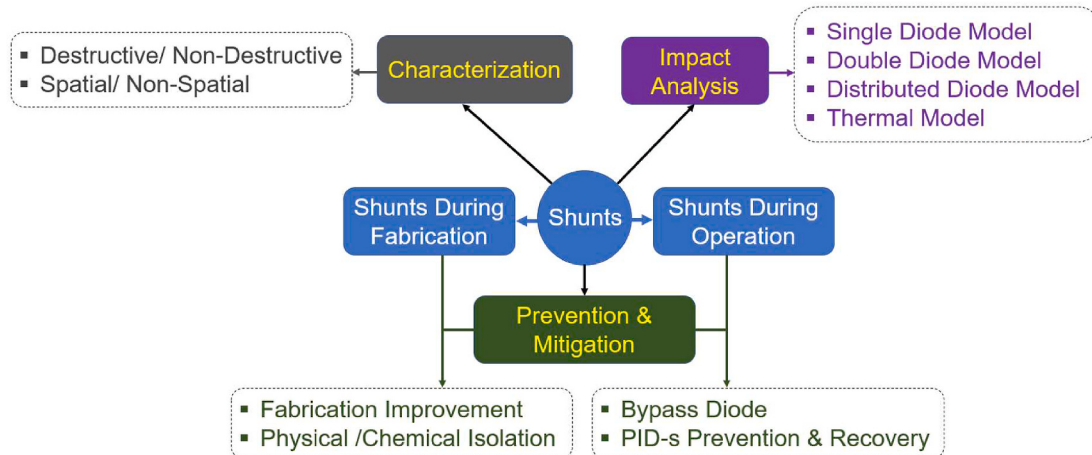


**Fig. 29.** Shunt types and their characterization, modeling approaches, and mitigation techniques.

larger area, making the removal of a large cell area unfeasible. Particularly, for PID-s, reverse recovery methods are available, yet achieving full recovery remains unattainable in the majority of instances. Hence, researchers are now focusing on prevention, considering it better than cure. Different encapsulant resistant to drift of Na ions are being considered as a potential strategy for PID-resistant PV modules.

- o **Main Issue:** Mitigation strategies vary depending on the type of shunt. Techniques like physical removal, bypass diodes, and reverse recovery methods have been explored, but challenges remain, particularly with PID-related shunts, where full recovery is often unattainable.
- o **Follow-up Research:** Researchers should focus more on preventive measures, such as developing encapsulant materials that resist Na ion drift, which is a key contributor to PID. Exploration of innovative bypass diode technologies and alternative strategies for mitigating complex shunt types should also be prioritized.

Addressing these challenges and exploring future research avenues will enhance PV technologies, ensuring increased efficiency, reliability, and longevity despite shunt-related issues. Shunts significantly impact PV performance, leading to reductions in FF,  $P_{max}$ , and  $V_{oc}$ , especially under low light conditions. Implementing preventive measures and refining module designs can mitigate the impact of shunts, and researchers should focus on real-time monitoring systems for shunt-related performance degradation.

## 7. Conclusion

This comprehensive review has provided an in-depth analysis of shunt defects and degradation in crystalline silicon solar cells, emphasizing their significant impact on cell performance, reliability, and long-term module stability.

- By categorizing shunt mechanisms and evaluating various characterization techniques, this work has underscored the importance of accurate and non-destructive diagnostic methods such as luminescence and lock-in thermography, which have emerged as powerful tools for both qualitative and quantitative analysis.
- In addition to characterization, this review has highlighted the need for precise modeling approaches to understand the spatial effects of shunts on solar cell performance. Various electrical and thermal models were evaluated, emphasizing their respective strengths and limitations in accurately predicting the impact of shunts. Currently, the distributed diode model offers the best accuracy but it is complex and requires more computational power.

- Furthermore, this work reviewed several mitigation techniques, noting their effectiveness in addressing shunt defects. Mitigation techniques such as chemical and physical isolation are most effective for point shunts, though they reduce the active area. For other shunts, such as PID, reverse biasing recovery during non-operational hours is the most effective, but complete recovery is not achieved in most cases. Therefore, challenges remain in improving their efficiency and applicability across different scenarios.

Despite advancements in understanding and mitigating shunts, opportunities for further research persist. These include optimizing characterization methods, developing more robust mitigation strategies, and exploring new materials and technologies. Overall, continued progress in these areas is crucial for enhancing the efficiency and reliability of solar cells, thereby supporting the broader adoption of solar energy as a sustainable power source.

## CRediT authorship contribution statement

**Ravi Kumar:** Writing – original draft, Visualization, Methodology, Investigation, Formal analysis, Data curation, Conceptualization.  
**Rajesh Gupta:** Writing – review & editing, Supervision, Resources, Project administration, Methodology, Conceptualization.

## Declaration of competing interest

The authors declare that they have no known competing financial interests or personal relationships that could have appeared to influence the work reported in this paper.

## Data availability

No data was used for the research described in the article.

## Acknowledgements

We gratefully acknowledge the support of the Prime Minister's Research Fellowship (PMRF) from the Ministry of Education, Government of India, which provided financial assistance during the tenure of this Ph.D. research.

## References

- [1] Share of electricity generated by renewables, Our World in Data, <https://ourworldindata.org/grapher/share-electricity-renewables>. (Accessed 31 January 2024).
- [2] "Solar PV," International Energy Agency (IEA). <https://www.iea.org/energy-systems/renewables/solar-pv> (accessed January 31, 2024).

- [3] K. Hasan, S. Yousuf, M. Tushar, B. Das, P. Das, M. Islam, Effects of different environmental and operational factors on the PV performance: a comprehensive review, *Energy Sci. Eng.* 10 (2) (2022) 656–675, <https://doi.org/10.1002/ese3.1043>.
- [4] J. Kim, M. Rabelo, S. Padi, H. Yousuf, E. Cho, J. Yi, A review of the degradation of photovoltaic modules for life expectancy, *Energies* 14 (2021) 4278, <https://doi.org/10.3390/en14144278>.
- [5] D. Jordan, S. Kurtz, Photovoltaic degradation rates—an analytical review, *Prog. Photovoltaics Res. Appl.* 21 (1) (2013) 12–29, <https://doi.org/10.1002/pip>.
- [6] V. Sharma, S. Chandel, Performance and degradation analysis for long term reliability of solar photovoltaic systems: a review, *Renew. Sustain. Energy Rev.* 27 (2013) 753–767, <https://doi.org/10.1016/j.rser.2013.07.046>.
- [7] M. Aghaei, et al., Review of degradation and failure phenomena in photovoltaic modules, *Renew. Sustain. Energy Rev.* 159 (2022) 112160, <https://doi.org/10.1016/j.rser.2022.112160>.
- [8] M. Köntges, et al., “IEA PVPS subtask 3.2: review of failures of photovoltaic modules,” paris [Online]. Available: <https://iea-pvps.org/key-topics/review-of-failures-of-photovoltaic-modules-final/>, 2014.
- [9] O. Breitenstein, J. Rakotonaina, M. Al Rifai, M. Werner, Shunt types in crystalline silicon solar cells, *Prog. Photovoltaics Res. Appl.* 12 (7) (2004) 529–538, <https://doi.org/10.1002/pip.544>.
- [10] A. Dhass, E. Natarajan, L. Ponnusamy, Influence of shunt resistance on the performance of solar photovoltaic cell, in: International Conference on Emerging Trends in Electrical Engineering and Energy Management (ICETEEM), 2012, pp. 382–386, <https://doi.org/10.1109/ICETEEM.2012.6494522>.
- [11] M. Barbato, M. Meneghini, A. Cester, G. Mura, E. Zanoni, G. Meneghesso, Influence of shunt resistance on the performance of an illuminated string of solar cells: theory, simulation, and experimental analysis, *IEEE Trans. Device Mater. Reliab.* 14 (4) (2014) 942–950, <https://doi.org/10.1109/TDMR.2014.2347138>.
- [12] P. Somasundaran, R. Gupta, Evaluation of shunt losses in industrial silicon solar cells, *Int. J. Photoenergy* 2016 (2016) 8029608, <https://doi.org/10.1155/2016/8029608>.
- [13] A. Luque, S. Hegedus, *Handbook of Photovoltaic Science and Engineering*, second ed., John Wiley & Sons, 2011.
- [14] O. Breitenstein, W. Eberhardt, K. Iwig, Imaging the local forward current density of solar cells by dynamical precision contact thermography, in: 1st World Conference on Photovoltaic Energy Conversion (WCPEC), 1994, pp. 1633–1636, <https://doi.org/10.1109/wcpec.1994.520530>.
- [15] M. Sarkar, Effect of various model parameters on solar photovoltaic cell simulation: a SPICE analysis, *Renewables* 3 (13) (2016), <https://doi.org/10.1186/s40807-016-0035-3>.
- [16] M. Islam, M. Rahaman, S. Mominuzzaman, The effect of Irradiation on different parameters of monocrystalline photovoltaic solar cell, in: 3rd International Conference on the Developments in Renewable Energy Technology (ICDRET), IEEE, 2014, pp. 1–6, <https://doi.org/10.1109/icdret.2014.6861716>.
- [17] O. Breitenstein, J. Rakotonaina, S. Neve, M. Al Rifai, M. Werner, Shunt types in multicrystalline solar cells, in: 3rd World Conference on Photovoltaic Energy Conversion (WCPEC), 2003, pp. 987–990.
- [18] O. Breitenstein, J. Bauer, J. Rakotonaina, Material-induced shunts in multicrystalline silicon solar cells, *Semiconductors* 41 (4) (2007) 440–443, <https://doi.org/10.1134/S106378260704015X>.
- [19] O. Breitenstein, et al., Lock-in thermography investigation of shunts in screen-printed and PERL solar cells, *Conf. Rec. IEEE Photovolt. Spec. Conf.* (2002) 430–433, <https://doi.org/10.1109/pvsc.2002.1190551>.
- [20] O. Breitenstein, Lock-in thermography for investigating solar cells and materials, *Quant. InfraRed Thermogr. J.* 7 (2) (2010) 147–165, <https://doi.org/10.3166/qirt.7.147-165>.
- [21] O. Breitenstein, M. Langenkamp, O. Lang, A. Schirrmacher, Shunts due to laser scribining of solar cells evaluated by highly sensitive lock-in thermography, *Sol. Energy Mater. Sol. Cells* 65 (1) (2001) 55–62, [https://doi.org/10.1016/S0927-0248\(00\)00077-5](https://doi.org/10.1016/S0927-0248(00)00077-5).
- [22] O. Breitenstein, A. Khanna, Y. Augarten, J. Bauer, J. Wagner, K. Iwig, Quantitative evaluation of electroluminescence images of solar cells, *Phys. Status Solidi Rapid Res. Lett.* 4 (1–2) (2010) 7–9, <https://doi.org/10.1002/pssr.200903304>.
- [23] O. Breitenstein, J. Rakotonaina, M. Rifai, Quantitative evaluation of shunts in solar cells by lock-in thermography, *Prog. Photovoltaics Res. Appl.* 11 (8) (2003) 515–526, <https://doi.org/10.1002/pip.520>.
- [24] O. Breitenstein, M. Langenkamp, K. McIntosh, C. Honsberg, M. Rinio, Localization of shunts across the floating junction of DSBC solar cells by lock-in thermography, in: 28th IEEE Photovoltaic Specialists Conference (PVSC), 2000, pp. 124–127, <https://doi.org/10.1109/PVSC.2000.915770>.
- [25] O. Breitenstein, J. Bauer, T. Trupke, R. Bardos, On the detection of shunts in silicon solar cells by photo- and electroluminescence imaging, *Prog. Photovoltaics Res. Appl.* 16 (2008) 325–330, <https://doi.org/10.1002/pip.803>.
- [26] E. Meyer, E. Dyk, The effect of reduced shunt resistance and shading on photovoltaic module performance, in: 31st IEEE Photovoltaic Specialists Conference (PVSC), 2005, pp. 1331–1334, <https://doi.org/10.1109/pvsc.2005.1488387>.
- [27] S. Pingel, et al., Potential induced degradation of solar cells and panels, in: 35th IEEE Photovoltaic Specialists Conference (PVSC), 2010, pp. 2817–2822, <https://doi.org/10.1109/PVSC.2010.5616823>.
- [28] V. Naumann, Microstructural Investigation of Pid-Shunts : Degradation and Recovery, 2014.
- [29] V. Naumann, C. Brzuska, M. Werner, S. Großer, C. Hagendorf, Investigations on the formation of stacking fault-like PID-shunts, *Energy Proc.* 92 (2016) 569–575, <https://doi.org/10.1016/j.egypro.2016.07.021>.
- [30] V. Naumann, PID-Shunting: Understanding from Nanoscale to Module Level, 2014, pp. 1–16.
- [31] V. Naumann, et al., Explanation of potential-induced degradation of the shunting type by Na decoration of stacking faults in Si solar cells, *Sol. Energy Mater. Sol. Cells* 120 (2014) 383–389, <https://doi.org/10.1016/j.solmat.2013.06.015>.
- [32] V. Naumann, D. Lausch, C. Hagendorf, Sodium decoration of PID-s crystal defects after corona induced degradation of bare silicon solar cells, *Energy Proc.* 77 (2015) 397–401, <https://doi.org/10.1016/j.egypro.2015.07.055>.
- [33] V. Naumann, C. Hagendorf, S. Grosser, M. Werner, J. Bagdahn, Micro structural root cause analysis of potential induced degradation in c-Si solar cells, *Energy Proc.* 27 (2012) 1–6, <https://doi.org/10.1016/j.egypro.2012.07.020>.
- [34] V. Naumann, et al., The role of stacking faults for the formation of shunts during potential-induced degradation of crystalline Si solar cells, *Phys. Status Solidi Rapid Res. Lett.* 7 (5) (2013) 315–318, <https://doi.org/10.1002/pssr.201307090>.
- [35] A. Sinha, M. Bliss, X. Wu, S. Roy, R. Gottschalg, R. Gupta, Cross-characterization for imaging parasitic resistive losses in thin-film photovoltaic modules, *J. Imaging* 2 (3) (2016) 1–19, <https://doi.org/10.3390/jimaging2030023>.
- [36] V. Puranik, R. Gupta, Analysis and insight of electroluminescence imaging in the assessment of potential-induced degradation in crystalline silicon photovoltaic module, *Eng. Fail. Anal.* 134 (Apr. 2022) 106027, <https://doi.org/10.1016/j.engfailanal.2022.106027>.
- [37] S.P. Harvey, et al., Investigating PID shunting in polycrystalline silicon modules via multiscale, multitechnique characterization, *Prog. Photovoltaics Res. Appl.* 26 (6) (2018) 377–384, <https://doi.org/10.1002/pip.2996>.
- [38] A. Humada, M. Hobraj, S. Mekhilef, H. Hamada, Solar cell parameters extraction based on single and double-diode models: a review, *Renew. Sustain. Energy Rev.* 56 (2016) 494–509, <https://doi.org/10.1016/j.rser.2015.11.051>.
- [39] S. Pannientakandi, R. Gupta, S. Manjoli, Effect of local shunting on the electrical mismatch losses in industrial silicon photovoltaic modules, *Int. J. Power Energy Res.* 2 (1) (2018) 1–15, <https://doi.org/10.22606/ijper.2018.21001>.
- [40] P. Somasundaran, R. Gupta, Influence of local shunting on the electrical performance in industrial Silicon solar cells, *Sol. Energy* 139 (2016) 581–590, <https://doi.org/10.1016/j.solener.2016.10.020>.
- [41] R. Gupta, P. Somasundaran, D. Nandi, Electrical simulation and characterization of shunts in solar cells, *Appl. Mech. Mater.* 110–116 (2012) 2453–2457. <http://10.4028/www.scientific.net/AMM.110-116.2453>.
- [42] M. Langenkamp, O. Breitenstein, Classification of shunting mechanisms in crystalline silicon solar cells, *Sol. Energy Mater. Sol. Cells* 72 (2002) 433–440, [https://doi.org/10.1016/S0927-0248\(01\)00191-X](https://doi.org/10.1016/S0927-0248(01)00191-X).
- [43] S. Roy, R. Gupta, Non-destructive approach for severity investigation of shunts in crystalline silicon photovoltaic modules by combination of electroluminescence imaging and lock-in thermography, *Meas. Sci. Technol.* 30 (2019) 044009, <https://doi.org/10.1088/1361-6501/ab0265>.
- [44] Y. Hu, High-resolution lock-in thermography investigation on industrial multicrystalline silicon solar cells, *IEEE J. Photovoltaics* 3 (3) (2013) 952–956, <https://doi.org/10.1109/JPHOTOV.2013.2255733>.
- [45] S. Tepner, A. Lorenz, Printing technologies for silicon solar cell metallization: a comprehensive review, *Prog. Photovoltaics Res. Appl.* 31 (6) (2023) 557–590, <https://doi.org/10.1002/pip.3674>.
- [46] J. Bai, Z. Zhang, J. Calata, G. Lu, Low-temperature sintered nanoscale silver as a novel semiconductor device-metallized substrate interconnect material, *IEEE Trans. Compon. Packag. Technol.* 29 (3) (2006) 589–593, <https://doi.org/10.1109/TCAPT.2005.853167>.
- [47] J. Fields, et al., The formation mechanism for printed silver-contacts for silicon solar cells, *Nat. Commun.* 7 (2016) 11143, <https://doi.org/10.1038/ncomms11143>.
- [48] S. Kumar, R. Meena, R. Gupta, Finger and interconnect degradations in crystalline silicon photovoltaic modules: a review, *Sol. Energy Mater. Sol. Cells* 230 (2021) 111296, <https://doi.org/10.1016/j.solmat.2021.111296>.
- [49] O. Breitenstein, J. Bauer, J. Wagner, A. Lotnyk, Imaging physical parameters of pre-breakdown Sites by lock-in Thermography Techniques, *Prog. Photovoltaics Res. Appl.* 16 (2008) 679–685, <https://doi.org/10.1002/pip.848>.
- [50] J.M. Wagner, J. Bauer, A. Lotnyk, O. Breitenstein, Pre-breakdown mechanisms in multicrystalline silicon solar cells, in: 23rd European Photovoltaic Solar Energy Conference (EUPVSEC), 2008, pp. 1164–1168.
- [51] O. Breitenstein, et al., Physical mechanisms of breakdown in multicrystalline silicon solar cells, in: 34th IEEE Photovoltaic Specialists Conference (PVSC), 2009, pp. 181–186, <https://doi.org/10.1109/PVSC.2009.5411700>.
- [52] J. Wagner, J. Bauer, O. Breitenstein, Classification of pre-breakdown phenomena in multicrystalline silicon solar cells, in: 24th European Photovoltaic Solar Energy Conference (EUPVSEC), 2009, pp. 925–929.
- [53] D. Lausch, et al., Identification of pre-breakdown mechanism of silicon solar cells at low reverse voltages, *Appl. Phys. Lett.* 97 (2010) 073506, <https://doi.org/10.1063/1.3480415>.
- [54] W. Kwapis, et al., Physical mechanisms of breakdown in multicrystalline silicon solar cells, in: 24th European Photovoltaic Solar Energy Conference (EUPVSEC), 2009, pp. 896–900.
- [55] K. Bothe, D. Hinken, K. Ramspeck, S. Herlufsen, J. Schmidt, R. Bredel, Imaging and analysis of pre-breakdown sites in multicrystalline silicon solar cells, in: 24th European Photovoltaic Solar Energy Conference (EUPVSEC), 2009, pp. 21–25.
- [56] J. Bauer, D. Lausch, H. Blumtritt, N. Zakharov, O. Breitenstein, Avalanche breakdown in multicrystalline solar cells due to preferred phosphorous diffusion

- at extended defects, *Prog. Photovoltaics Res. Appl.* 21 (2013) 1444–1453, <https://doi.org/10.1002/pip>.
- [57] O. Breitenstein, Understanding shunting mechanisms in silicon cells: a review, in: 17th Workshop on Crystalline Silicon Solar Cells and Modules: Materials and Processes, 2007, pp. 139–144 [Online]. Available: <http://www.ncbi.nlm.nih.gov/pubmed/7429637>.
- [58] P. Grunow, S. Krauter, T. Buseth, S. Wendlandt, A. Drobisch, Hot spot risk analysis on silicon cell modules, in: 5th World Conference on Photovoltaic Energy Conversion (WCPEC), 2010, pp. 4002–4006, <https://doi.org/10.4229/25thEUPVSEC2010-4AV.3.13>.
- [59] J. Torres, S. Nashih, C. Fernandes, J. Leite, The effect of shading on photovoltaic solar panels, *Energy Syst.* 9 (2018) 195–208, <https://doi.org/10.1007/s12667-016-0225-5>.
- [60] E. Meyer, E. Dyk, Assessing the reliability and degradation of photovoltaic module performance parameters, *IEEE Trans. Reliab.* 53 (1) (2004) 83–92, <https://doi.org/10.1109/TR.2004.824831>.
- [61] H. Kawamura, et al., Simulation of I-V characteristics of a PV module with shaded PV cells, *Sol. Energy Mater. Sol. Cells* 75 (2003) 613–621, [https://doi.org/10.1016/S0927-0248\(02\)00134-4](https://doi.org/10.1016/S0927-0248(02)00134-4).
- [62] H. Hanif, M. Pander, B. Jaekel, J. Schneider, A. Bakhtiari, W. Maier, A novel electrical approach to protect PV modules under various partial shading situations, *Sol. Energy* 193 (2019) 814–819, <https://doi.org/10.1016/j.solener.2019.10.035>.
- [63] M. Santhakumari, N. Sagar, A review of the environmental factors degrading the performance of silicon wafer-based photovoltaic modules: failure detection methods and essential mitigation techniques, *Renew. Sustain. Energy Rev.* 110 (2019) 83–100, <https://doi.org/10.1016/j.rser.2019.04.024>.
- [64] A. Ndiaye, A. Charki, A. Kobi, C. Kébé, P. Ndiaye, V. Sambou, Degradations of silicon photovoltaic modules: a literature review, *Sol. Energy* 96 (2013) 140–151, <https://doi.org/10.1016/j.solener.2013.07.005>.
- [65] I. Höiaas, K. Grujic, A. Imenes, I. Burud, E. Olsen, N. Belbachir, Inspection and condition monitoring of large-scale photovoltaic power plants: a review of imaging technologies, *Renew. Sustain. Energy Rev.* 161 (2022) 112353, <https://doi.org/10.1016/j.rser.2022.112353>.
- [66] P. Hacke, et al., System voltage potential-induced degradation mechanisms in PV modules and methods for test, in: 37th IEEE Photovoltaic Specialists Conference (PVSC), 2011, pp. 814–820, <https://doi.org/10.1109/PVSC.2011.6186079>.
- [67] N.G. Dhere, N. Shiradkar, E. Schneller, Evolution of leakage current paths in MC-Si PV modules from leading manufacturers undergoing high-voltage bias testing, *IEEE J. Photovoltaics* 4 (2) (2014) 654–658, <https://doi.org/10.1109/JPHOTOV.2013.2294764>.
- [68] T. Kim, N. Park, D. Kim, The effect of moisture on the degradation mechanism of multi-crystalline silicon photovoltaic module, *Microelectron. Reliab.* 53 (2013) 1823–1827, <https://doi.org/10.1016/j.micrel.2013.07.047>.
- [69] J. Cueto, T. McMahon, Analysis of leakage currents in photovoltaic modules under high-voltage bias, *Prog. Photovoltaics Res. Appl.* 10 (2002) 15–28, <https://doi.org/10.1002/pip.401>.
- [70] M. Islam, M. Hasanuzzaman, N. Rahim, Effect of different factors on the leakage current behavior of silicon photovoltaic modules at high voltage stress, *IEEE J. Photovoltaics* 8 (5) (2018) 1259–1265, <https://doi.org/10.1109/JPHOTOV.2018.2841500>.
- [71] R. Kumar, M. Kumar, R. Gupta, Leakage current in solar photovoltaic modules, in: *Solar Energy: Advancements and Challenges*, 2023, pp. 111–123, <https://doi.org/10.1201/9781003373902-7>.
- [72] H. Miranda, L. Costa, S. Soares, J. Silva, Potential induced degradation (PID): review, in: *IEEE PES Transmission and Distribution Conference and Exhibition (T & D LA)*, 2020, pp. 1–6, <https://doi.org/10.1109/TDLA47668.2020.9326184>.
- [73] L. Koester, S. Lindig, A. Louwen, A. Astigarraga, G. Manzolini, D. Moser, Review of photovoltaic module degradation, field inspection techniques and techno-economic assessment, *Renew. Sustain. Energy Rev.* 165 (2022) 112616, <https://doi.org/10.1016/j.rser.2022.112616>.
- [74] C. Molto, et al., Review of potential-induced degradation in bifacial PV modules, *Energy Technol.* 11 (4) (2023) 2200943, <https://doi.org/10.1002/ente.202200943>.
- [75] H. Wang, et al., Potential-induced degradation: recombination behavior, temperature coefficients and mismatch losses in crystalline silicon photovoltaic power plant, *Sol. Energy* 188 (2019) 258–264, <https://doi.org/10.1016/j.solener.2019.06.023>.
- [76] W. Luo, et al., Potential-induced degradation in photovoltaic modules: a critical review, *Energy Environ. Sci.* 10 (2017) 43–68, <https://doi.org/10.1039/c6ee02271e>.
- [77] J. Šlamberger, M. Schwark, B. Aken, P. Virtič, Comparison of potential-induced degradation (PID) of n-type and p-type silicon solar cells, *Energy* 161 (2018) 266–276, <https://doi.org/10.1016/j.energy.2018.07.118>.
- [78] K. Arekar, V. Puranik, R. Gupta, Performance analysis of PID affected crystalline silicon PV module under partial shading condition, in: 48th IEEE Photovoltaic Specialists Conference (PVSC), 2021, pp. 2415–2420, <https://doi.org/10.1109/PVSC43889.2021.9518533>.
- [79] R. Kumar, V. Puranik, R. Gupta, Application of electroluminescence imaging to distinguish ohmic and non ohmic shunting in inaccessible cells within a PV module, *IEEE J. Photovoltaics* 14 (2) (2024) 296–304, <https://doi.org/10.1109/JPHOTOV.2024.3357210>.
- [80] N. Dong, M. Islam, Y. Ishikawa, Y. Uraoka, The influence of sodium ions decorated micro-cracks on the evolution of potential induced degradation in p-type crystalline silicon solar cells, *Sol. Energy* 174 (2018) 1–6, <https://doi.org/10.1016/j.solener.2018.08.082>.
- [81] S. Harvey, J. Aguiar, P. Hacke, H. Guthrey, S. Johnston, M. Al-Jassim, Sodium accumulation at potential-induced degradation shunted areas in polycrystalline silicon modules, *IEEE J. Photovoltaics* 6 (6) (Nov. 2016) 1440–1445, <https://doi.org/10.1109/JPHOTOV.2016.2601950>.
- [82] B. Ziebarth, M. Mrovec, C. Elsässer, P. Gumbisch, Potential-induced degradation in solar cells: electronic structure and diffusion mechanism of sodium in stacking faults of silicon, *J. Appl. Phys.* 116 (9) (2014) 093510, <https://doi.org/10.1063/1.4894007>.
- [83] A. Bouaichi, et al., Experimental investigation of potential induced degradation (PID) impact and recovery on crystalline photovoltaic systems, 1st International Conference on Electronic Engineering and Renewable Energy (ICEERE) 519 (2018) 623–629, <https://doi.org/10.1007/978-981-13-1405-6>.
- [84] K. Sporleder, V. Naumann, J. Bauer, D. Hevisov, M. Turek, C. Hagendorf, Time-resolved investigation of transient field effect passivation states during potential-induced degradation and recovery of bifacial silicon solar cells, *Sol. RRL* 5 (7) (2021), <https://doi.org/10.1002/solr.202100140>.
- [85] J. Oh, S. Bowden, G. Tamizhmani, Potential-induced degradation (PID): incomplete recovery of shunt resistance and quantum efficiency losses, *IEEE J. Photovoltaics* 5 (6) (2015) 1540–1548, <https://doi.org/10.1109/JPHOTOV.2015.2459919>.
- [86] D. Lausch, et al., Sodium outdiffusion from stacking faults as root cause for the recovery process of potential-induced degradation (PID), *Energy Proc.* 55 (2014) 486–493, <https://doi.org/10.1016/j.egypro.2014.08.013>.
- [87] S. Großer, et al., Shunt analysis in solar cells - electro-optical classification and high resolution defect diagnostics, *Energy Proc.* 27 (2012) 7–12, <https://doi.org/10.1016/j.egypro.2012.07.021>.
- [88] J. Carstensen, G. Popkirov, J. Bahr, H. Föll, CELLO: an advanced LBIC measurement technique for solar cell local characterization, *Sol. Energy Mater. Sol. Cells* 76 (4) (2003) 599–611, [https://doi.org/10.1016/S0927-0248\(02\)00270-2](https://doi.org/10.1016/S0927-0248(02)00270-2).
- [89] J. Carstensen, A. Schütt, G. Popkirov, H. Föll, CELLO measurement technique for local identification and characterization of various types of solar cell defects, *Phys. Status Solidi Curr. Top. Solid State Phys.* 8 (4) (2011) 1342–1346, <https://doi.org/10.1002/pssc.201083997>.
- [90] A. Heide, A. Schönecker, G. Wyers, W. Sinke, Mapping of contact resistance and locating shunts on solar cells using resistance analysis by mapping of potential (RAMP) techniques, in: 16th European Photovoltaic Solar Energy Conference (EUPVSEC), 2000, pp. 1438–1442.
- [91] G. Trentadue, D. Pavanello, E. Salis, M. Field, H. Müllejans, Determination of internal series resistance of PV devices: repeatability and uncertainty, *Meas. Sci. Technol.* 27 (5) (2016), <https://doi.org/10.1088/0957-0233/27/5/055005>.
- [92] M. Bliss, T. Betts, R. Gottschalch, Indoor measurement of photovoltaic device characteristics at varying irradiance, temperature and spectrum for energy rating, *Meas. Sci. Technol.* 21 (11) (2010), <https://doi.org/10.1088/0957-0233/21/11/115701>.
- [93] I. Konovalov, O. Breitenstein, K. Iwig, Local current-voltage curves measured thermally (LIVT): a new technique of characterizing PV cells, *Sol. Energy Mater. Sol. Cells* 48 (1997) 53–60, [https://doi.org/10.1016/S0927-0248\(97\)00069-X](https://doi.org/10.1016/S0927-0248(97)00069-X).
- [94] O. Breitenstein, M. Langenkamp, Quantitative local analysis of IV characteristics of solar cells by thermal methods, in: 2nd World Conference on Photovoltaic Energy Conversion (WCPEC), 1998, pp. 1382–1385.
- [95] K. Bothe, K. Ramspeck, D. Hinken, R. Brendel, Imaging techniques for the analysis of silicon wafers and solar cells, *ECS Trans.* 16 (6) (2008) 63–78, <https://doi.org/10.1149/1.2980293>.
- [96] C. Ballif, S. Peters, J. Isenberg, S. Riepe, D. Borchert, Shunt imaging in solar cells using low cost commercial liquid crystal sheets, in: 29th IEEE Photovoltaic Specialists Conference (PVSC), 2002, pp. 446–449, <https://doi.org/10.1109/pvsc.2002.1190555>.
- [97] J. Schmidt, I. Dierking, Localization and imaging of local shunts in solar cells using polymer-dispersed liquid crystals, *Prog. Photovoltaics Res. Appl.* 9 (4) (2001) 263–271, <https://doi.org/10.1002/pip.378>.
- [98] J. Rakotonaina, M. Rifai, O. Breitenstein, Quantitative analysis of the influence of shunts in solar cells by means of lock-in thermography, in: 3rd World Conference on Photovoltaic Energy Conversion (WCPEC), 2003, pp. 1065–1068, <https://doi.org/10.21611/qirt.2004.004>.
- [99] S. Huth, O. Breitenstein, A. Huber, D. Dantz, U. Lambert, F. Altmann, Lock-in IR-Thermography - a novel tool for material and device, in: *Diffusion and Defect Data Part B Solid State Phenomena*, 1999, pp. 741–746.
- [100] R. Gupta, O. Breitenstein, Unsteady-state lock-in thermography—application to shunts in solar cells, *Quant. InfraRed Thermogr. J.* 4 (1) (2007) 85–105, <https://doi.org/10.3166/qirt.4.85-105>.
- [101] O. Breitenstein, W. Warta, M. Langenkamp, Lock-in Thermography: Basics and Use for Evaluating Electronic Devices and Materials, Springer, Berlin, Heidelberg, 2010, <https://doi.org/10.1007/978-3-642-02417-7>.
- [102] S. Kumar, P. Jena, A. Sinha, R. Gupta, Application of infrared thermography for non-destructive inspection of solar photovoltaic module, *J. Non Destr. Test. Eval.* 6 (2017) 25–32.
- [103] O. Breitenstein, et al., Lock-in thermography- A universal tool for local analysis of solar cells, in: 20th European Photovoltaic Solar Energy Conference (EUPVSEC), 2005, pp. 590–593.
- [104] O. Breitenstein, S. Sturm, Lock-in thermography for analyzing solar cells and failure analysis in other electronic components, *Quant. InfraRed Thermogr. J.* 16 (3–4) (2019) 203–217, <https://doi.org/10.1080/17686733.2018.1563349>.
- [105] T. Fuyuki, H. Kondo, Y. Kaji, A. Ogane, Y. Takahashi, Analytic findings in the electroluminescence characterization of crystalline silicon solar cells, *J. Appl. Phys.* 101 (2) (2007) 1–5, <https://doi.org/10.1063/1.2431075>.

- [106] T. Fuyuki, A. Kitayanan, Photographic diagnosis of crystalline silicon solar cells utilizing electroluminescence, *Appl. Phys. Mater. Sci. Process* 96 (1) (2009) 189–196, <https://doi.org/10.1007/s00339-008-4986-0>.
- [107] T. Trupke, B. Mitchell, J. Weber, W. McMillan, R. Bardos, R. Kroese, Photoluminescence imaging for photovoltaic applications, *Energy Proc.* 15 (2012) 135–146, <https://doi.org/10.1016/j.egypro.2012.02.016>.
- [108] M. Kasemann, et al., Luminescence imaging for the detection of shunts on silicon solar cells, *Prog. Photovoltaics Res. Appl.* 16 (2008) 297–305, <https://doi.org/10.1002/pip.812>.
- [109] O. Breitenstein, et al., Can luminescence imaging replace lock-in thermography on solar cells and wafers? *IEEE J. Photovoltaics* 1 (2) (2011) 159–167, <https://doi.org/10.1109/vpsc.2011.6185846>.
- [110] O. Breitenstein, et al., Luminescence imaging versus lock-in thermography on solar cells and wafers, in: 26th European Photovoltaic Solar Energy Conference and Exhibition, 2011, pp. 1031–1038, <https://doi.org/10.1109/JPHOTOV.2011.2169394>.
- [111] M. Abbott, T. Trupke, H. Hartmann, R. Gupta, O. Breitenstein, Laser isolation of shunted regions in industrial solar cells, *Prog. Photovoltaics Res. Appl.* 15 (7) (2007) 613–620, <https://doi.org/10.1002/pip.766>.
- [112] E. Sugimura, S. Takamoto, S. Tsujii, K. Hirata, A. Tani, T. Fuyuki, Spatially resolved electroluminescence imaging of shunt sources in crystalline silicon solar cells, *Jpn. J. Appl. Phys.* 51 (10) (2012) 10NA02, <https://doi.org/10.1143/JJAP.51.10NA02>.
- [113] V. Puranik, R. Kumar, R. Gupta, Generalized quantitative electroluminescence method for the performance evaluation of defective and unevenly degraded crystalline silicon photovoltaic module, *Prog. Photovoltaics Res. Appl.* 31 (3) (2023) 269–282, <https://doi.org/10.1002/pip.3632>.
- [114] M. Islam, M. Hasanuzzaman, N. Rahim, Investigation of the potential induced degradation on site-aged polycrystalline PV modules operating in Malaysia, *Measurement* 119 (May 2017) (2018) 283–294, <https://doi.org/10.1016/j.measurement.2018.01.061>.
- [115] V. Puranik, R. Gupta, Novel quantitative electroluminescence method for detailed performance analysis of PID-s affected crystalline silicon PV module, *IEEE J. Photovoltaics* 11 (6) (Nov. 2021) 1470–1478, <https://doi.org/10.1109/JPHOTOV.2021.3108764>.
- [116] E. Marstein, et al., Shunt detection and characterization with fluorescent microthermal imaging, in: 4th World Conference on Photovoltaic Energy Conversion (WCPEC), 2006, pp. 1107–1110, <https://doi.org/10.1109/WCPEC.2006.279354>.
- [117] O. Breitenstein, Nondestructive local analysis of currentvoltage characteristics of solar cells by lock-in thermography, *Sol. Energy Mater. Sol. Cells* 95 (10) (2011) 2933–2936, <https://doi.org/10.1016/j.solmat.2011.05.049>.
- [118] Y. Augarten, et al., Calculation of quantitative shunt values using photoluminescence imaging, *Prog. Photovoltaics Res. Appl.* 21 (2012) 933–941, <https://doi.org/10.1002/pip.2180>.
- [119] S. Roy, P. Somasundaran, R. Gupta, Estimation of shunt resistance by electroluminescence imaging, in: 29th European Photovoltaic Solar Energy Conference and Exhibition, 2014, pp. 1224–1227.
- [120] S. Roy, R. Gupta, Quantitative estimation of shunt resistance in crystalline silicon photovoltaic modules by electroluminescence imaging, *IEEE J. Photovoltaics* 9 (6) (2019) 1741–1747, <https://doi.org/10.1109/JPHOTOV.2019.2930402>.
- [121] V. Puranik, R. Gupta, Standardized applications of electroluminescence imaging for efficient investigation of potential-induced degradation shunting in crystalline silicon photovoltaic module, *Sol. Energy* 245 (2022) 183–192, <https://doi.org/10.1016/j.solener.2022.09.014>.
- [122] R. Kumar, V. Puranik, R. Gupta, Unveiling the potential of infrared thermography in quantitative investigation of potential-induced degradation in crystalline silicon PV module, *Sol. Energy Adv.* 4 (2024) 100049, <https://doi.org/10.1016/j.seja.2023.100049>.
- [123] R. Kumar, V. Puranik, R. Gupta, Application of infrared thermography for cell-level power estimation of PID-s impacted crystalline silicon PV module, *IEEE J. Photovoltaics* 13 (1) (2023) 141–149, <https://doi.org/10.1109/JPHOTOV.2022.3229485>.
- [124] M. Green, Accurate expressions for solar cell fill factors including series and shunt resistances, *Appl. Phys. Lett.* 108 (8) (2016), <https://doi.org/10.1063/1.4942660>.
- [125] M. Loulou, M. Turkestan, N. Brahmi, M. Abdelkrim, Current dependence of series and shunt resistances of solar cells, in: 9th International Renewable Energy Congress (IREC), 2018, pp. 1–5, <https://doi.org/10.1109/IREC.2018.8362494>.
- [126] M. Barbato, et al., Effect of shunt resistance on the performance of mc-Silicon solar cells: a combined electro-optical and thermal investigation, in: 38th IEEE Photovoltaic Specialists Conference (PVSC), 2012, pp. 1241–1245, <https://doi.org/10.1109/PVSC.2012.6317827>.
- [127] S. Rummel, T. McMahon, Effect of cell shunt resistance on PV module performance at reduced light levels, 13th NREL Photovoltaics Program Review Meeting 581 (1996) 581–586, <https://doi.org/10.1063/1.49388>.
- [128] D. Rossi, M. Omana, D. Giaffreda, C. Metra, Modeling and detection of hotspot in shaded photovoltaic cells, *IEEE Trans. Very Large Scale Integr. Syst.* 23 (6) (2015) 1031–1039, <https://doi.org/10.1109/TVLSI.2014.2333064>.
- [129] H. Mehta, H. Warke, K. Kukadiya, A. Panchal, Accurate expressions for single-diode-model solar cell parameterization, *IEEE J. Photovoltaics* 9 (3) (2019) 803–810, <https://doi.org/10.1109/JPHOTOV.2019.2896264>.
- [130] Y. Mahmoud, W. Xiao, Evaluation of shunt model for simulating photovoltaic modules, *IEEE J. Photovoltaics* 8 (6) (2018) 1818–1823, <https://doi.org/10.1109/JPHOTOV.2018.2869493>.
- [131] K. Ishaque, Z. Salam, H. Taheri, Simple, fast and accurate two-diode model for photovoltaic modules, *Sol. Energy Mater. Sol. Cells* 95 (2) (2011) 586–594, <https://doi.org/10.1016/j.solmat.2010.09.023>.
- [132] E. Dyk, E. Meyer, Analysis of the effect of parasitic resistances on the performance of photovoltaic modules, *Renew. Energy* 29 (3) (2004) 333–344, [https://doi.org/10.1016/S0960-1481\(03\)00250-7](https://doi.org/10.1016/S0960-1481(03)00250-7).
- [133] A. Zekry, A. Al-Mazroo, A distributed SPICE-model of a solar cell, *IEEE Trans. Electron. Dev.* 43 (5) (1996) 691–700, <https://doi.org/10.1109/16.491244>.
- [134] D. Giaffreda, et al., Local shunting in multicrystalline silicon solar cells: distributed electrical simulations and experiments, *IEEE J. Photovoltaics* 4 (1) (2014) 40–47, <https://doi.org/10.1109/JPHOTOV.2013.2280838>.
- [135] P. Somasundaran, M. Shilpi, R. Gupta, Evaluation of mismatch losses due to shunts in industrial silicon photovoltaic modules, in: 7th International Conference on Environment and Industrial Innovation, vol. 67, 2017 012013, <https://doi.org/10.1088/1755-1315/67/1/012013>.
- [136] C. Buerhop, D. Schlegel, M. Niess, C. Vodermayer, R. Weißmann, C. Brabec, Reliability of IR-imaging of PV-plants under operating conditions, *Sol. Energy Mater. Sol. Cells* 107 (2012) 154–164, <https://doi.org/10.1016/j.solmat.2012.07.011>.
- [137] P. Botsaris, J. Tsanakas, Infrared thermography as an estimator technique of a photovoltaic module performance via operating temperature measurements, in: 10th ECNDT Conference, 2010, pp. 1–11.
- [138] T. Kaden, K. Lammers, H. Möller, Power loss prognosis from thermographic images of PID affected silicon solar modules, *Sol. Energy Mater. Sol. Cells* 142 (Nov. 2015) 24–28, <https://doi.org/10.1016/j.solmat.2015.05.028>.
- [139] M. Björn, H. Laura, A. Alfons, K. Klaus, R. Christian, Yield predictions for photovoltaic power plants:empirical validation,recent advances and remaining uncertainties, *Prog. Photovoltaics Res. Appl.* 24 (4) (2016) 570–583, <https://doi.org/10.1002/pip.2616>.
- [140] M. Florides, A. Livera, G. Makrides, G. Georgiou, Shunt resistance relation to power loss due to potential induced degradation in crystalline photovoltaic cells, in: 46th IEEE Photovoltaic Specialists Conference, 2019, pp. 1950–1954, <https://doi.org/10.1109/PVSC40753.2019.8980722>.
- [141] A. Sinha, O. Sastry, R. Gupta, Nondestructive characterization of encapsulant discoloration effects in crystalline-silicon PV modules, *Sol. Energy Mater. Sol. Cells* 155 (2016) 234–242, <https://doi.org/10.1016/j.solmat.2016.06.019>.
- [142] N. Baghel, N. Chander, Performance comparison of mono and polycrystalline silicon solar photovoltaic modules under tropical wet and dry climatic conditions in east-central India, *Clean Energy* 6 (2022) 165–177, <https://doi.org/10.1093/cz/kac001>.
- [143] T. Buonassisi, et al., Assessing the role of transition metals in shunting mechanisms using synchrotron-based techniques, in: 3rd World Conference on Photovoltaic Energy Conversion (WCPEC), 2003, pp. 1120–1123.
- [144] A. Hauser, et al., Comparison of different techniques for edge isolation, in: 17th European Photovoltaic Solar Energy Conference (EUPVSEC), 2001, pp. 1739–1742.
- [145] O. Haupt, et al., Improved laser edge isolation of crystalline silicon solar cells using a high power picosecond laser, in: International Laser Safety Conference, 2009, pp. 1181–1187, <https://doi.org/10.2351/1.5061471>.
- [146] D. Chithambaranadan, V. Veeramuthu, Q. Nguyen, T. Lommasson, R. Goldberg, T. Bostrom, Efficiency improvement in nonprime crystalline silicon solar cells by chemical isolation of shunts under front metallization, *IEEE J. Photovoltaics* 5 (1) (2015) 206–211, <https://doi.org/10.1109/JPHOTOV.2014.2373815>.
- [147] S. Silvestre, A. Boronat, A. Choudier, Study of bypass diodes configuration on PV modules, *Appl. Energy* 86 (9) (2009) 1632–1640, <https://doi.org/10.1016/j.apenergy.2009.01.020>.
- [148] R. Vieira, F. Araújo, M. Dhimish, M. Guerra, A comprehensive review on bypass diode application on photovoltaic modules, *Energies* 13 (2020) 2472, <https://doi.org/10.3390/en13102472>.
- [149] K. Kim, P. Krein, Reexamination of photovoltaic hot spotting to show inadequacy of the bypass diode, *IEEE J. Photovoltaics* 5 (5) (2015) 1435–1441, <https://doi.org/10.1109/JPHOTOV.2015.2444091>.
- [150] G. Spagnolo, P. Vecchio, G. Makary, D. Papalillo, A. Martoccia, A review of IR thermography applied to PV systems, in: 11th International Conference on Environment and Electrical Engineering (EEEIC), 2012, pp. 879–884, <https://doi.org/10.1109/EEEIC.2012.6221500>.
- [151] H. Nagel, A. Metz, K. Wangemann, Crystalline Si solar cells and modules featuring excellent stability against potential-induced degradation, in: 26th European Photovoltaic Solar Energy Conference (EUPVSEC), 2011, pp. 3107–3112.
- [152] Y. Augarten, et al., Detection and isolation of localised shunts in industrial silicon solar cells using, *Sol. Energy* (2007) 1220–1223.
- [153] H. Hao, S. Zhong, X. Zhang, W. Shen, Optimization of shunt isolation processing for silicon solar cells via laser and chemical etching, *Appl. Surf. Sci.* 311 (2014) 870–875, <https://doi.org/10.1016/j.apsusc.2014.05.078>.
- [154] L. Zhang, H. Shen, Z. Yang, J. Jin, Shunt removal and patching for crystalline silicon solar cells using infrared imaging and laser cutting, *Prog. Photovoltaics Res. Appl.* 18 (1) (2010) 54–60, <https://doi.org/10.1002/pip.934>.